Med

CellPress

Article

Closed-loop automated drug infusion regulator: A clinically translatable, closed-loop drug delivery system for personalized drug dosing

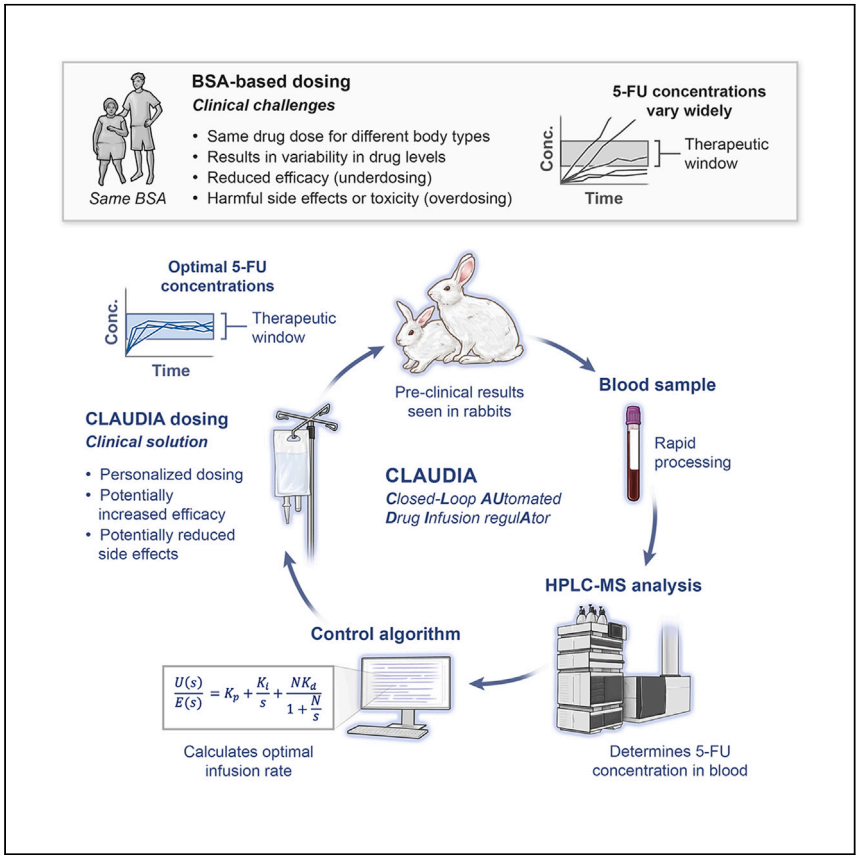

Chemotherapy dosing is based on a patient's body surface area, which ignores many sources of pharmacokinetic variability, leading to toxicities or lack of efficacy. DeRidder et al. developed a clinically translatable, closed-loop system that measures the drug concentration and changes the infusion rate of drug to maintain the target concentration.

Foundational Research

Louis B. DeRidder, Kyle A. Hare, Aaron Lopes, ..., Douglas A. Rubinson, Robert Langer, Giovanni Traverso

cgt20@mit.edu

Highlights

Current dosing can result in pharmacokinetic variability and worse patient outcomes

CLAUDIA is a closed-loop drug delivery system that can personalize drug dosing

CLAUDIA uses high-performance liquid chromatography mass spectrometry as its sensor

CLAUDIA controls 5-fluorouracil levels *in vivo* under clinically relevant conditions

DeRidder et al., Med 5, 780–796
July 12, 2024
https://doi.org/10.1016/j.medj.2024.03.020

CellPress

Med

Article

Closed-loop automated drug infusion regulator: A clinically translatable, closed-loop drug delivery system for personalized drug dosing

Louis B. DeRidder,[1,2,3,4] Kyle A. Hare,[2,5] Aaron Lopes,[2,4] Josh Jenkins,[2,3] Nina Fitzgerald,[2,4] Emmeline MacPherson,[6] Niora Fabian,[2,3,7] Josh Morimoto,[2,4] Jacqueline N. Chu,[2,8,9,16] Ameya R. Kirtane,[2,4] Wiam Madani,[2,3] Keiko Ishida,[2,3,4] Johannes L.P. Kuosmanen,[2,3] Naomi Zecharias,[2,3,6] Christopher M. Colangelo,[10] Hen-Wei Huang,[2,3,4] Makaya Chilekwa,[2] Nikhil B. Lal,[3,4,11] Shriya S. Srinivasan,[2,4] Alison M. Hayward,[2,3,4,7] Brian M. Wolpin,[8,12,13] David Trumper,[3] Troy Quast,[14] Douglas A. Rubinson,[8,12,13] Robert Langer,[1,2,5,15] and Giovanni Traverso[2,3,4,17,*]

SUMMARY

Background: Dosing of chemotherapies is often calculated according to the weight and/or height of the patient or equations derived from these, such as body surface area (BSA). Such calculations fail to capture intra- and interindividual pharmacokinetic variation, which can lead to order of magnitude variations in systemic chemotherapy levels and thus under- or overdosing of patients.

Methods: We designed and developed a closed-loop drug delivery system that can dynamically adjust its infusion rate to the patient to reach and maintain the drug's target concentration, regardless of a patient's pharmacokinetics (PK).

Findings: We demonstrate that closed-loop automated drug infusion regulator (CLAUDIA) can control the concentration of 5-fluorouracil (5-FU) in rabbits according to a range of concentration-time profiles (which could be useful in chronomodulated chemotherapy) and over a range of PK conditions that mimic the PK variability observed clinically. In one set of experiments, BSA-based dosing resulted in a concentration 7 times above the target range, while CLAUDIA keeps the concentration of 5-FU in or near the targeted range. Further, we demonstrate that CLAUDIA is cost effective compared to BSA-based dosing.

Conclusions: We anticipate that CLAUDIA could be rapidly translated to the clinic to enable physicians to control the plasma concentration of chemotherapy in their patients.

Funding: This work was supported by MIT's Karl van Tassel (1925) Career Development Professorship and Department of Mechanical Engineering and the Bridge Project, a partnership between the Koch Institute for Integrative Cancer Research at MIT and the Dana-Farber/Harvard Cancer Center.

CONTEXT AND SIGNIFICANCE

Chemotherapies are commonly dosed based on a patient's body surface area (BSA) or weight, which fails to account for the many other sources of pharmacokinetic variability between patients. These sources of pharmacokinetic variability are ignored in standard clinical practice and can result in suboptimal dosing, which can reduce efficacy and increase toxicity. The authors have developed a medical device that could enable physicians to control the concentration of the drugs in their patient's blood regardless of the many factors that could alter the pharmacokinetics for a patient. This medical device could potentially be rapidly translated to the clinic, where it may be able to decrease the toxicity and increase the efficacy of chemotherapies given to patients.

INTRODUCTION

While the modalities for treating cancer have advanced significantly over the past decade, the method of dosing chemotherapeutics has not changed, and as a result, the concentration of chemotherapeutic drugs in patients' blood can vary widely,

which could lead to worse therapeutic outcomes.[1–6] To date, chemotherapies are typically dosed based on body surface area (BSA), which is a measure of the surface area of a person's body. Clinically, BSA is commonly estimated based on the patient's height and weight. Dosing on a BSA basis does not take into account interindividual variabilities in pharmacokinetics (PK) in patients with the same BSA (Figure 1A).[1–4] Moreover, within the same patient, the concentration of drug in the blood can vary significantly during a constant rate infusion; in some patients, the concentration of a drug can vary over a 10-fold range due to circadian-rhythm-induced changes in the expression of the drug-metabolizing enzyme (Figure 1A).[7] Thus, even within the same patient, the concentration of a drug can be 3 times lower than the target concentration at one point during an infusion and over 3 times higher than the target at another time during the same infusion. The DuBois and DuBois formula for calculating the ideal BSA based on a patient's height and weight was developed in 1916 by empirically fitting data from only nine people, and it is still used clinically today.[5] Moreover, the DuBois and DuBois formula was further simplified into the widely used Mosteller formula for estimating BSA in a highly cited NEJM paper in 1987, which results in additional variation to the BSA estimate in the DuBois and DuBois formula.[8]

The PK and pharmacodynamics for many chemotherapies have widespread variability due to a range of factors, including circadian effects, genetic polymorphisms, and microbiome and food effects, as well as sex differences, as has been reviewed previously.[6,9–15] The result of BSA-based dosing is that patients may be overdosed or underdosed, resulting in toxicity or lack of efficacy, respectively. Moreover, chemotherapy-induced toxicity can cause patients to switch, delay, or stop their cancer treatment. Unfortunately, underdosing is often not recognized clinically and thus could lead to tumor growth or metastasis.[1–4] This highlights the need to develop an intervention that can maintain the plasma concentration of drugs within its therapeutic window.

Multiple commercial assays have been developed that enable determination of the blood concentration of chemotherapeutic agents to inform how to adjust the dose for the next treatment cycle.[1,3,4,16] This procedure is called therapeutic drug monitoring (TDM). In these assays, blood is sampled from a patient one or two times during a treatment regimen, manually processed, and analyzed using high-performance liquid chromatography-mass spectrometry (HPLC-MS) or an immunoassay, such as the My5-FU (5-fluorouracil) assay.[17] Indeed, Kline et al. demonstrated that patients receiving TDM of 5-FU had higher disease-free survival rates and fewer side effects compared to patients dosed via BSA.[3] Additionally, phase 2 and 3 clinical trials have also shown the benefit of TDM over BSA-based dosing.[18,19]

However, despite the utility of TDM, it is rarely used when administering chemotherapies.[1] TDM is time and labor intensive and requires healthcare workers to sample blood at regular intervals, quantify the drug concentration, and then adjust the infusion rate. Additionally, TDM does not account for circadian changes in drug concentration, as blood is sampled during normal working hours. Thus, there is an unmet clinical need for a device that can alter the infusion rate of chemotherapeutic agents automatically. A closed-loop system measures the blood concentration of the drug and changes the infusion rate to keep the concentration of the drug within the drug's therapeutic window (Figure 1B).[20–25] Closed-loop drug delivery devices have already reached the clinic for other disease states: the artificial pancreas system for type II diabetes is the best-known example.[20–24] Herein, we describe a closed-loop system that can control the concentration of 5-FU *in vivo*. Although we perform multiple components of closed-loop automated drug infusion regulator (CLAUDIA)

[1]Harvard-MIT Division of Health Science Technology, Massachusetts Institute of Technology, Cambridge, MA 02139, USA

[2]David H. Koch Institute for Integrative Cancer Research, Massachusetts Institute of Technology, Cambridge, MA 02139, USA

[3]Department of Mechanical Engineering, Massachusetts Institute of Technology, Cambridge, MA 02139, USA

[4]Division of Gastroenterology, Hepatology, and Endoscopy, Brigham and Women's Hospital, Harvard Medical School, Boston, MA 02115, USA

[5]Department of Chemical Engineering, Massachusetts Institute of Technology, Cambridge, MA 02139, USA

[6]Department of Biological Engineering, Massachusetts Institute of Technology, Cambridge, MA 02139, USA

[7]Division of Comparative Medicine, Massachusetts Institute of Technology, Cambridge, MA 02139, USA

[8]Harvard Medical School, Boston, MA 02115, USA

[9]Division of Gastroenterology, Massachusetts General Hospital, Boston, MA 02114, USA

[10]Agilent Technologies, Lexington, MA 02421, USA

[11]MIT Media Lab, Massachusetts Institute of Technology, Cambridge, MA 02139, USA

[12]Department of Medical Oncology, Dana-Farber Cancer Institute, Boston, MA 02215, USA

[13]Department of Medicine, Brigham and Women's Hospital, Boston, MA 02115, USA

[14]College of Public Health, University of South Florida, Tampa, FL 33612, USA

[15]Department of Surgery, Boston Children's Hospital, Harvard Medical School, Boston, MA 02115, USA

[16]Present address: Integrated Gastroenterology Consultants, North Chelmsford, MA 01863, USA

[17]Lead contact

*Correspondence: cgt20@mit.edu

https://doi.org/10.1016/j.medj.2024.03.020

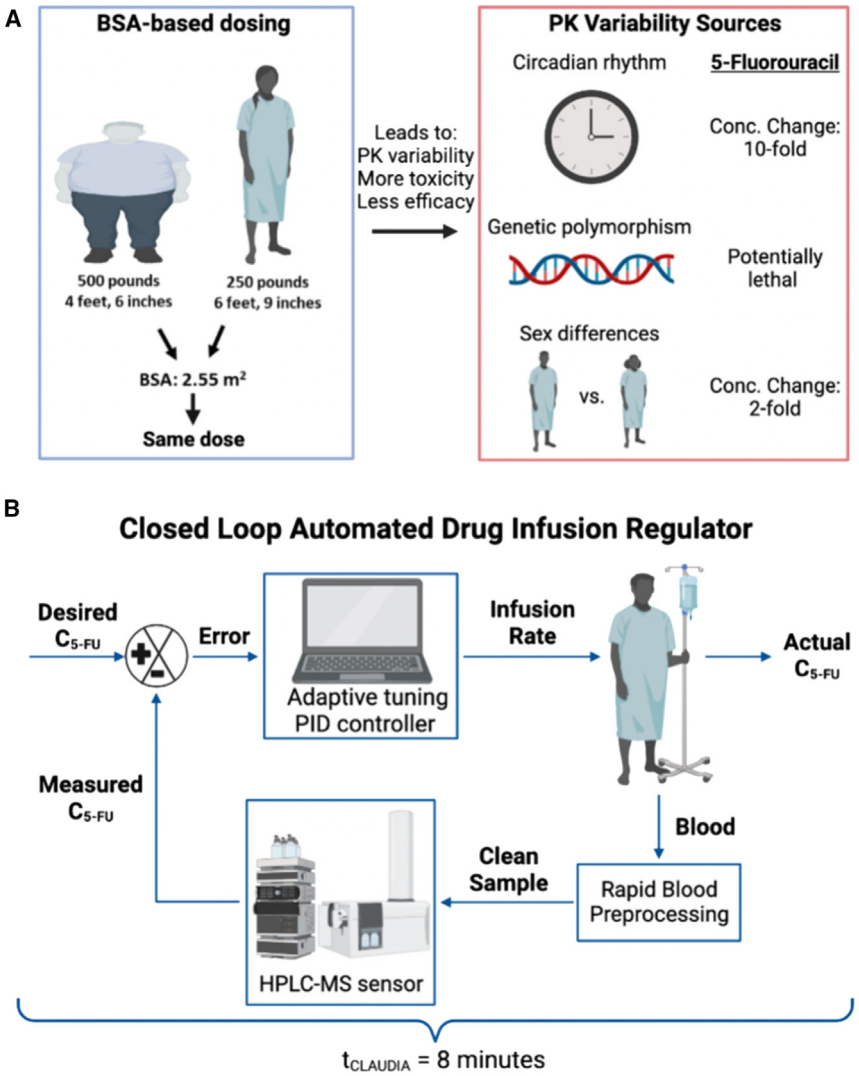

Figure 1. CLAUDIA seeks to address the shortfalls of dosing chemotherapies on a BSA basis

(A) Two patients with the same ideal BSA receive the same dose of chemotherapy even if many other physiological differences exist between them. The resulting imprecision results in PK variability and subsequent underdosing that results in lack of efficacy and overdosing, which results in toxicities.

(B) An overview of CLAUDIA. Blood is withdrawn from the patient and is then rapidly processed to be suitable to be placed onto HPLC-MS for analysis. The HPLC-MS determines the concentration of drug (e.g., 5-FU) in the blood of the patient, and the control algorithm determines the updated infusion rate of drug for the patient based upon the error, which is the difference between the current measured and desired concentration of the drug.

(A) is adapted from DeRidder et al.[6]

manually in this present work, each step could potentially be fully automated using commercially available devices, thereby enabling fully autonomous, closed-loop control of drug concentrations.

RESULTS

Overview of CLAUDIA

CLAUDIA is a closed-loop system capable of being rapidly translated to the clinic due to its use of commercially available components. CLAUDIA takes blood from

the patient and performs rapid sample preparation of blood to extract the drug, which enables the drug's concentration to be measured using HPLC-MS (Figure 1B).[26,27] The measured concentration of the drug is then input into a control algorithm, which compares the current concentration with the target concentration (i.e., computes the error) and then adjusts the infusion rate of the drug to keep its concentration within the therapeutic window. A proportional-integral-derivative (PID) controller with a derivative filter was selected as the control algorithm for our system, as PID controllers are simple, highly versatile, and proven to be effective for our application.[25,28] HPLC-MS was chosen to monitor the therapeutic drug level and determine the PK profile because HPLC-MS can resolve and identify target analytes in complex bioanalytical matrices, as described previously.[1,29]

We selected 5-FU as our model drug to evaluate the performance of CLAUDIA, as closed-loop control of 5-FU concentrations could have large clinical benefit due to multiple reasons. First, it has been widely used in clinical practice to treat gastrointestinal, head and neck, and breast cancers and remains the third most commonly used chemotherapeutic drug in the world for solid cancers.[3,30,31] Second, there is large interpatient and intrapatient variability in the PK of 5-FU, which can be lethal in some patients (Figure 1A).[32–38] About 80% of 5-FU is metabolized by the hepatic enzyme dihydropyrimidine dehydrogenase (DPD), and there is genotypic variation in DPYD (the gene encoding DPD) within the population.[1–3,39–42] Individuals with different genotypes of DPYD metabolize 5-FU at different rates, which results in different PK profiles among individuals; patients with two non-functional DPYD alleles are at a larger risk of experiencing lethal 5-FU overdoses.[4] Indeed, the toxicities due to homozygous mutation in DPYD can lead to death, which led the US Food and Drug Administration (FDA) to approve uridine triacetate (tradename: Vistogard) for patients who receive an otherwise fatal overdose of 5-FU.[43,44] DPD activity also follows a circadian rhythm, and as a result, a patient receiving a continuous infusion can experience a 10-fold fluctuation of 5-FU concentrations in the course of a single infusion (Figure 1A).[7,32–34] Importantly, while there is a genetic test available for screening the DPYD genotype, it is not performed routinely, and it only takes into account the 3–4 most prevalent DPYD alleles that correlate with 5-FU toxicity.[36] These DPYD genotype tests thus neglect the multiple additional DPYD alleles that impact 5-FU PK and the additional genes that impact 5-FU outcomes. Moreover, there are no DPYD phenotype assays available that are practical to use clinically. Third, 5-FU has a short average half-life (8–22 min) in most patients, making it highly amenable to control via a closed-loop system.[35] And finally, it is dosed by infusion for 10 to 46 h, thus potentially providing a significant amount of time for the patient to experience clinical benefit from CLAUDIA keeping the concentration in the therapeutic window.[30,40,45]

Development and validation of the rapid sample preparation and HPLC-MS method

After the blood is collected from the patient, the drug must be extracted from the blood before the concentration of the drug can be determined via HPLC-MS.[26] Traditional sample preparation processes—such as solid-phase extraction, liquid-liquid extraction, and cleanup via affinity chromatography—take between 30 and 60 min, which is too long to be used in our closed-loop system, because the longer the time between sampling blood and measuring the drug concentration, the worse the closed-loop system is able to control the levels of drug in the patient.[46] Thus, we developed a rapid sample preparation process that takes 130 $\pm$ 3 s (n = 24) and gives a clear filtrate (Figures S1A and S1C). In this process, blood is centrifuged to separate plasma from the blood cells, and the supernatant is mixed with a 25/75

methanol/acetonitrile (v/v) mixture, vortexed, centrifuged, and filtered before being placed on the HPLC-MS. We additionally developed a 4 min HPLC-MS method to minimize the time between taking the sample and receiving a concentration measurement. We used an Agilent high-resolution, time-of-flight (TOF) MS to enable us to accurately detect 5-FU concentrations using our rapid sample preparation method, as dozens of molecules that were extracted from the blood elute simultaneously from the HPLC. The system was able to clearly resolve 5-FU from interferences that differed only by 50–100 ppm (Data S1 Figure 1). Using a control sample, the mass error was confirmed to be less than 2 ppm for 5-FU with a resolving power of >7,000.

The sample preparation and HPLC-MS methods were validated for selectivity and specificity, sensitivity, accuracy, precision, recovery, and stability by directly referencing the FDA industry guide for bioanalytical method development and validation (Tables S1A, S2A, and S2B; Figure S2; Data S1 Figure 1).[47] Our method validation results demonstrated that we obtained a linear calibration curve from 0.5 to 40 mg/L, which covers the clinically relevant concentration range, including the target range of 2.5–3 mg/L (Figure S2; Table S1A).[18] Our inter-day accuracy and precision (in terms of percent coefficient of variation) were both under 15% at all concentrations except the lower limit of quantification (LLOQ) of 0.5 m/L, which had an inter-day precision of 22.5% (Tables S1A, S2A, and S2B). Our sample preparation process resulted in 11.7% $\pm$ 2.4% and 20.6% $\pm$ 2.8% recovery at the low and high levels of our method validation, respectively (Figure S1A). CLAUDIA's sensing system is sensitive and selective, as sample chromatograms demonstrate that 5-FU and 5-bromouracil (5-BU) were not detected in clean blood processed by CLAUDIA's sensing system but were detected when the blood was spiked (Data S1 Figure 1). We additionally performed a partial validation of an alternative, more rapid sample preparation procedure (Figure S1B), and we found it was accurate and precise over a linear range including the clinically relevant concentration range of 5-FU (Table S1B). In sum, we successfully developed a method to rapidly determine the concentration of 5-FU using HPLC-MS as the sensor.

Setpoint experiments

Once we had developed CLAUDIA, we compared its performance to BSA-based dosing to bring the concentration of 5-FU to the clinically determined optimal concentration of 5-FU for humans (2.5–3.0 mg/L) in six different rabbits (Figures 2A–2F).[18] We first administered 5-FU as a continuous rate infusion (CRI) whose rate was determined by the BSA of the rabbit and modeled the PK profile of 5-FU using a first-order model of the data (Figures 2A–2C, S3A, and S3B). We used these data to model our system in SIMULINK to determine the controller gains that would enable CLAUDIA to perform well under a range of scenarios, as described in the STAR Methods. In the BSA-based dosing group, the concentration at steady state ranged from 2.5 to 6 mg/L (Figures 2A–2C), while all CLAUDIA groups reached the target of 2.5–3 mg/L at steady state (Figures 2D–2F). Qualitatively, it was clear that the adjustments of the infusion rate by CLAUDIA (Figures S4A–S4C) allowed the system to maintain the concentration of 5-FU closer to the target concentration compared to the BSA-based group (Figures 2A–2F and S5C). Moreover, the percentages of time within the target window were, on average, 45% $\pm$ 3% for the CLAUDIA group versus 13% $\pm$ 18% for the BSA-based dosing group (Figure 2H, not statistically significant). CLAUDIA resulted in an area under the curve (AUC) within the target range for all three experiments, while BSA-based dosing resulted in no experiments being in the target range, with one group being under the target and two being above the target range (Figure 2I, not statistically significant). These results demonstrate that

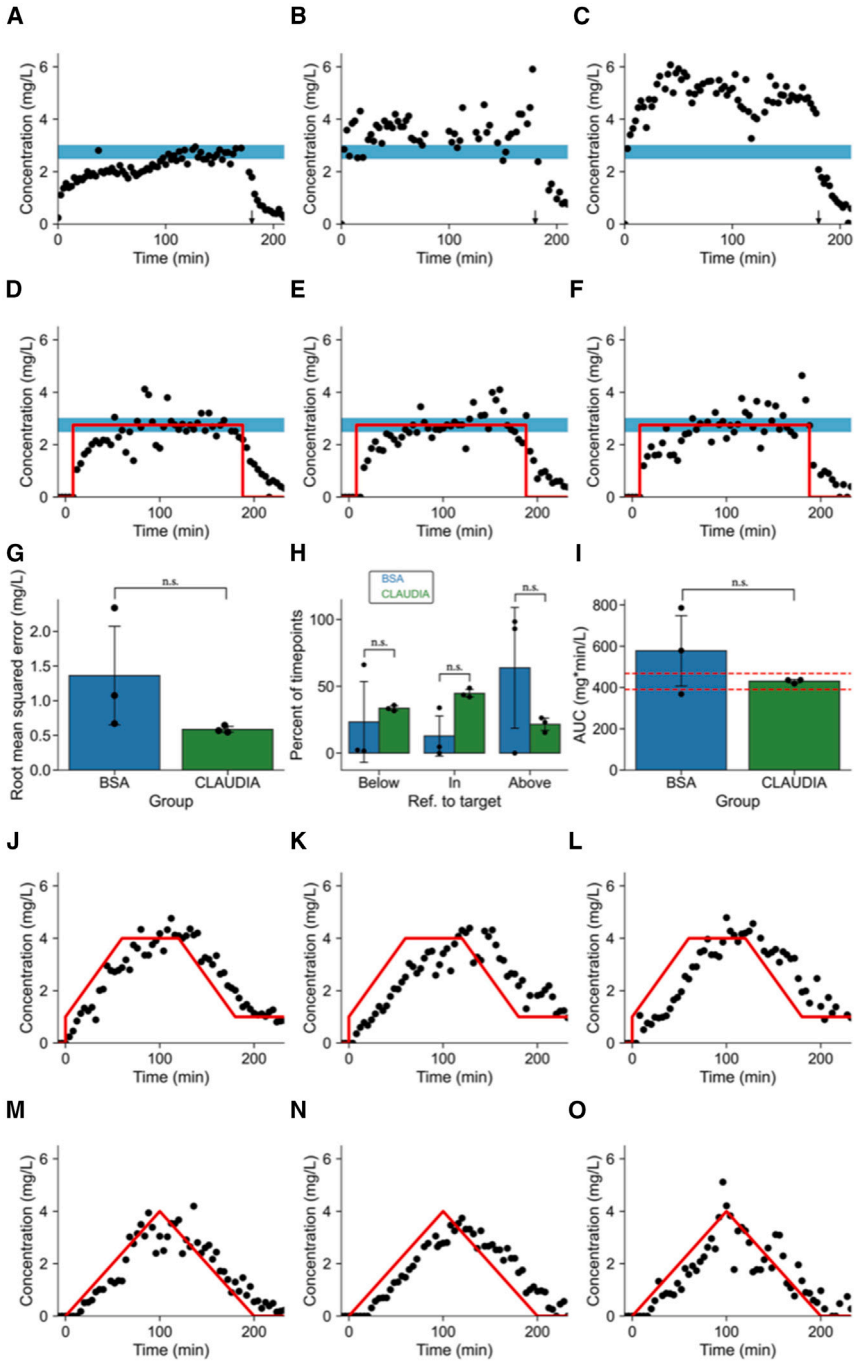

Figure 2. CLAUDIA can control the concentration of 5-FU *in vivo* according to multiple concentration-time profiles

(A–C) Control group dosed by BSA. 5-FU was given as a continuous rate infusion from time 0 to 180 min (the end of infusion is depicted with the arrow) (n = 3 different rabbits).

(D–F) Performance of CLAUDIA in controlling 5-FU concentrations according to a step function (red line) (n = 3 different rabbits).

(A–F) The optimal therapeutic window for 5-FU is depicted in the shaded blue region.

(G) Root-mean-squared error from the target concentration of 2.75 mg/L for the BSA and CLAUDIA groups.

(H) Percentage of time points of the BSA and CLAUDIA groups spent below, in, and above the target concentration.

Figure 2. *Continued*
(I) Area under the curve (AUC) for the BSA and CLAUDIA groups. The target AUC range is depicted by the two horizontal lines.
(J–O) Performance of CLAUDIA in controlling the concentration according to the (J–L) trapezoidal-like shape and (M–O) tent-like shape.
In all images, the target concentration profile is shown by the red line, and the actual data are demonstrated by the black datapoints. Data are shown as the mean ± standard deviation. Independent Student's t test. n.s., no significance.

CLAUDIA is capable of both increasing the amount of time that 5-FU is within the target concentration and decreasing the extent that the concentration varies from the target concentration when it is out of range. The concentration-time curves in the CLAUDIA experiments (Figure 2) were similar to the curves given in the simulations (Figure S3C), demonstrating that our SIMULINK model captures CLAUDIA's performance and the PK of the rabbit well. Moreover, the initial infusion rate for the CLAUDIA groups was set to 0 μL/s to enable us to understand the dynamics of the control system, while the BSA group started and ended at the infusion rate based upon the rabbit's BSA. If it was necessary for the concentration to reach the target concentration quicker in the CLAUDIA group, then the initial infusion rate could be set to the BSA dose or another infusion rate that is optimal for the performance.

After evaluating CLAUDIA's ability to bring the concentration of 5-FU to the target concentration in a step function concentration-time profile, we also evaluated its ability to change the concentration of 5-FU according to additional concentration-time profiles (Figures 2J–2O). 5-FU, like many other chemotherapies, has been shown to have differences in effectiveness in killing cancer cells as a function of the time of day the chemotherapy is given to the patient.[48–50] Thus, we investigated CLAUDIA's ability to control the concentration of 5-FU in two different concentration-time profiles, which could be used clinically to give 5-FU via a chronomodulated schedule, and demonstrated that CLAUDIA could control the concentration of 5-FU according to both trapezoid-like and tent-like shaped concentration-time profiles (Figures 2J–2O) by adjusting its infusion rate (Figures S4D–S4I).

Disturbance experiments

We next sought to investigate whether CLAUDIA could still control the levels of 5-FU when the PK was pharmacologically altered during the experiment. To achieve this goal, we administered (E)-5-(2-bromovinyl)uracil, an inhibitor to DPD, the enzyme that metabolizes 5-FU (Figure 3A).[35] Indeed, by giving this inhibitor orally 1.5 h before a 5-FU bolus, we were able to alter its PK (Figures S5A and S5B). We next performed a preliminary experiment to study the impact of the DPD inhibitor on a CRI of 5-FU by administering the DPD inhibitor 1 h into the experiment (Data S1 Figures 2A and 2B). This experiment demonstrated that the increase in 5-FU half-life occurs approximately 90 min after the administration of the DPD inhibitor (Data S1 Figure 2B).

Additionally, we performed an experiment with CLAUDIA after administering the DPD inhibitor at time 1 h. We used the same control algorithm that we used for the setpoint experiments and found that the concentration-time profile began to demonstrate oscillations, which indicates that the DPD inhibitor altered the PK of the rabbit enough to cause the controller to no longer be able to function properly (Data S1 Figures 2C and 2D). Specifically, the gain in the rabbit's PK (i.e., the concentration of 5-FU in the blood for a given infusion rate of 5-FU) increased significantly to cause the system to become unstable. Thus, we decided to implement an adaptive tuning approach, where the controller gains (k_p, k_I, k_d) were reduced by a gain factor,

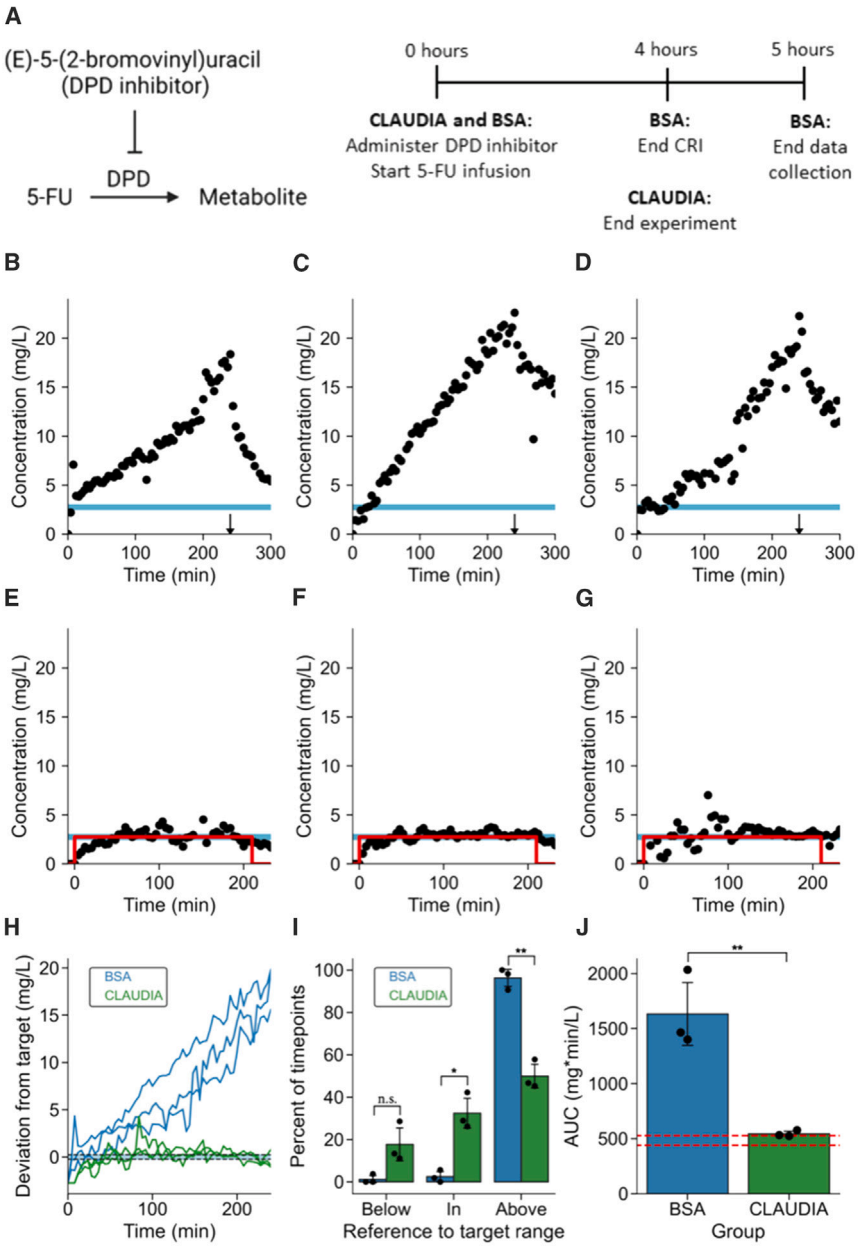

Figure 3. Disturbance experiments demonstrate the ability of CLAUDIA to control 5-FU concentrations in the presence of a disturbance

(A) (Left) An inhibitor to DPD (the enzyme that metabolizes 5-FU) was administered to rabbits orally to alter the PK of 5-FU in rabbits in order to capture the PK variability of 5-FU seen clinically and to challenge our system with a disturbance. (Right) The experimental layout for both the BSA-based dosing and CLAUDIA groups. The DPD inhibitor was administered orally at time 0 min for both groups.

(B–D) For the control, BSA-based group, 5-FU was given for 4 h as a CRI on a BSA basis, and then the concentration of 5-FU continued to be measured for the following hour after 5-FU was no longer infused into the rabbit (n = 3 independent rabbits). The arrow denotes when the CRI was stopped.

(E–G) The concentration-time profile for the CLAUDIA group (n = 3 independent rabbits). The target concentration of 5-FU is given by the red line.

(B–G) The blue shaded region represents the target concentration range.

(H) Deviation from the target concentration of 2.75 mg/L.

Figure 3. *Continued*
(I and J) The (I) percentage of time points in range and (J) 5-FU AUC for the BSA-based dosing and CLAUDIA groups.
CRI, continuous rate infusion. Data are shown as the mean ± standard deviation. Independent Student's t test. n.s., not significant. *$p < 0.05$ and **$p < 0.01$. Bonferroni correction applied to (I) ($n = 3$ tests).

depending on if the concentration of 5-FU exceeded a predetermined threshold for two different time points during the treatment regimen (Table 1). These gain factors were determined by understanding that the steady-state concentration is directly proportional to the system's gain; we originally planned to apply a proportional gain factor to counteract these increases in controller gain (e.g., if the concentration exceeds the target concentration 2-fold, then the gain-factor would be ½). After performing simulations for these situations, we decided to make the gain factors slightly stronger, as shown in Table 1 (e.g., the gain factor of ½ was applied to concentrations over 5 mg/L instead of 5.5 mg/L).

We decided to give the inhibitor at time 0 min during further experiments (Figure 3A) so that CLAUDIA would be tested both under nominal conditions during the first 60–90 min of the experiment and in the presence of a disturbance to the system during the remaining 150–180 min. When we administered 5-FU as a CRI according to this scheme, we observed that the concentration of 5-FU was >18 mg/L in all experimental groups and reached a maximum concentration of 22 mg/L in two groups (Figures 3B–3D), which is over 15 mg/L above the target concentration range of 2.5–3 mg/L. Importantly, 5-FU reached the target concentration range when dosed on a BSA basis when given as a CRI without the DPD inhibitor (Figure 2A). Significantly, the variation in 5-FU PK with and without the DPD inhibitor replicates the >8-fold variability of 5-FU observed clinically.[39] Since it appears that the concentration of 5-FU was still increasing at the end of the CRI + DPD experiments (Figures 3B–3D), the actual steady-state concentration is likely higher than that reached during our experiment. Thus, our estimated 8-fold variability in 5-FU PK experienced in the rabbits in our studies with and without the DPD inhibitor may actually be larger what is observed clinically, which would show that CLAUDIA can perform well over a larger range of conditions that what is needed clinically.

While all experiments in the BSA-based dosing group reached concentrations of >18 mg/L when the DPD inhibitor was added (target: 2.5–3 mg/L), when we allowed CLAUDIA to control the concentration of 5-FU, the concentration of 5-FU only exceeded 7 mg/L at one time point, and it did not exceed 5 mg/L at any other time points (Figures 3E–3G and S5E–S5G). Overall, the CLAUDIA group deviated much less from the target range than the BSA-based group (Figures 3H and S5D). CLAUDIA increased the time in range from 2.50% ± 2.89% in the BSA-based group to 32.43% ± 8.58% (Figure 3I). Lastly, the AUC was decreased from 1,632.9 ± 348.5 mg min/L in the BSA-based group to 544.6 ± 28.2 mg min/L in the CLAUDIA group (target: 440–528 mg min/L) (Figure 3J). CLAUDIA decreased the flow rate of 5-FU as a function of time to keep the concentration of 5-FU within the target range, demonstrating that the ability to stay within the target range was due to the action of the controller (Figures S4J–S4L). Importantly, the adaptive tuning method prevented the third disturbance CLAUDIA experiment from becoming unstable (Figures 3G and S5G). Indeed, the system was beginning to experience unstable oscillations, but after the adaptive control algorithm went into effect, the system stabilized, and the concentration monotonically returned to the target range.

Table 1. Gain factors that are applied to the controller gains if a concentration threshold was exceeded twice during the experiment

If concentration exceeds (mg/L):	Gain factor
4	3/4
5	1/2
6	1/3
9	1/5
12	1/10

Cost-utility analysis

We next performed a cost-utility analysis (CUA) of CLAUDIA compared to both BSA-based dosing and TDM-guided dosing by developing a Markov cohort model of patients with metastatic colorectal cancer receiving 5-FU combination therapy (Figure 4A). Our model found TDM to be the cost-effective strategy at the efficiency frontier with an incremental cost-effectiveness ratio (ICER) of $79,000 per quality-adjusted life year (QALY) compared to BSA (Figure 4B; Data S1 Figure 3). CLAUDIA was the most effective strategy and yielded an increase of 0.33 QALY above TDM but had an ICER of $120,700/QALY compared to TDM, which was above the willingness-to-pay threshold of $100,000/QALY. However, TDM has not been well adopted in the clinic.[51] Therefore, we also performed a separate analysis of CLAUDIA compared to BSA only, which found that CLAUDIA was cost effective compared to BSA with an ICER of $92,500/QALY (Figure 4B). This suggests that the estimated cost per cycle of chemotherapy using CLAUDIA is cost effective compared to standard practice. The largest sources of uncertainty in our CUA model were the impact of CLAUDIA on oncologic outcomes (overall survival, progression-free survival) and toxicities—because CLAUDIA has not been tested in clinical trials—as well as the device cost. Thus, we then performed one-way sensitivity analyses of significant parameter inputs of the model, and we found that changes in the cost of CLAUDIA, utility of being on first-line therapy, relative risk of overall survival for patients on CLAUDIA compared to TDM, cost of BSA strategy, and utility of being in the progressed state all caused CLAUDIA to become cost ineffective compared to BSA-based dosing for some of the values of the parameters included in the sensitivity analysis but only at an ICER of up to $140,000/QALY (Data S1 Figure 4A). Lastly, we performed a one-way sensitivity analysis on the cost of CLAUDIA to find when it becomes cost effective compared to the TDM group with a cost-effectiveness threshold of $100,000/QALY. We found that if the cost of using CLAUDIA was about $100 less than our base case per cycle of chemotherapy, then it would be cost effective compared to TDM.

CLAUDIA can detect multiple chemotherapies simultaneously

One of the key benefits of using HPLC-MS as our sensor is that it can be directly applied to multiple other chemotherapies, which could enable CLAUDIA to control the concentration of other drugs independently as well as multiple drugs simultaneously.[26] To demonstrate the ability of CLAUDIA to detect the concentration of multiple drugs simultaneously, we spiked theophylline, thiotepa, cyclophosphamide, irinotecan, and doxorubicin together into blood and performed the same sample preparation technique that was optimized for 5-FU. We then analyzed the concentration of the drugs with a 3.5-min HPLC-MS method that was developed for detecting these multiple chemotherapies simultaneously. The results demonstrate that we can measure the concentrations of multiple chemotherapies simultaneously using our rapid sample preparation and HPLC-MS method (Table S2C; Data S1 Figure 7). We spiked blood with multiple chemotherapies mixed together and the

A

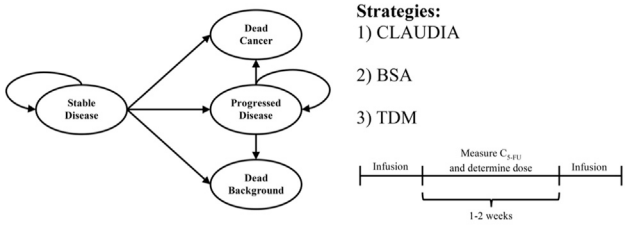

B

Strategy	Cost (USD)	Effectiveness (QALY)	ICER (USD/QALY)	ICER compared to BSA (USD/QALY)
BSA	67,900	1.64	-	-
TDM	121,300	2.31	79,100	79,100
CLAUDIA	160,100	2.64	120,700	92,500

Figure 4. Cost-utility model comparing cost effectiveness of BSA, therapeutic drug monitoring, and CLAUDIA approaches for 5-FU dosing

(A) State-transition diagram showing the health states and transitions in the model.

(B) Cost-effectiveness results. ICER, incremental cost effectiveness ratio.

multiple drugs individually to investigate whether mixing all the drugs together altered the ability to measure the concentration of the drug accurately and found that spiking multiple drugs together did not decrease the accuracy of the sensor.

DISCUSSION

Many chemotherapies are dosed on a BSA basis, which leads to significant PK variability and worse clinical outcomes due to the multiple factors that contribute to a drug's PK that BSA-based methods of dosing chemotherapies do not capture (e.g., genetic polymorphisms, circadian effects, renal/hepatic impairment, etc.).[6,9–15] In response, we developed CLAUDIA, which is capable of keeping the concentration of 5-FU within the therapeutic window under a range of PK conditions (Figures 2 and 3). Previous closed-loop systems that used novel aptamer electrochemical-based sensors tailored to specific chemotherapies enabled the concentration of the chemotherapy being administered to the animals to be detected and the concentration in the blood to be controlled by adjusting the infusion rate of the drug into the animal.[25,28] CLAUDIA's use of HPLC-MS as the sensor—which is the industry standard for PK analysis of small-molecule organic compounds in patients—and other components that are commercially available could enable the rapid translation of CLAUDIA to the clinic. Additionally, the ability of HPLC-MS to detect multiple different compounds may enable CLAUDIA to be applied to control the concentration of multiple different drugs either individually or in combination.[47]

CLAUDIA demonstrated the ability to control the concentration of 5-FU in a variety of settings, including for multiple different concentration-time profiles and in the presence of a disturbance that mimicked the PK variability observed clinically for 5-FU (Figures 2 and 3).[39] Indeed, while dosing 5-FU on a BSA basis resulted in PK variability, CLAUDIA brought the concentration of the drug near the target concentration in all experiments, where the concentration reached the clinically determined optimal concentration range for 5-FU (2.5–3.0 mg/L) (Figures 2A–2F and 3B–3G). It is important to note that one experiment in the BSA group (Figure 2A) performed similarly to the experiments in the CLAUDIA group in terms of percentage of time in range (Figure 2H); however, it underperformed in terms of AUC compared to CLAUDIA (Figure 2I).[18] This underscores the fact that if a clinician guesses the dose of chemotherapy correctly, then the concentration-time profile for that patient

can be within the target range according to some metrics. However, CLAUDIA consistently gave approximately the same average deviation from target and percentage of time in range among all three groups, demonstrating its ability to keep the concentration of a drug within the target window regardless of the exact PK differences. The adaptive tuning method allowed CLAUDIA to control the concentration of 5-FU even when the PK of the rabbit was altered significantly in a manner that modeled patients who do not metabolize 5-FU well (Figure 3). Future versions of the controller could also be further improved by implementing a more complex algorithm to detect the presence of oscillations in the system for use in the adaptive control algorithm, such as using the integral of absolute error.[52]

We next sought to determine the cost effectiveness of implementing CLAUDIA clinically by developing a CUA model and found that CLAUDIA is cost effective compared to BSA. When comparing all three strategies (BSA, TDM, and CLAUDIA), the cost-effectiveness analysis found TDM to be the cost-effective strategy. However, despite its performance in our model and its advantages, TDM is not commonly used in clinical practice, suggesting there are additional costs that were not captured by our analysis—for example, inconvenience/labor intensiveness for staff and patients. Additionally, compared to TDM, CLAUDIA had an ICER of $120,000/QALY. This is very close to the standard willingness-to-pay threshold of $100,000/QALY, and many have suggested that the willingness-to-pay threshold should be increased to $100,000–150,000/QALY, especially for cancer therapeutics.[53] Current clinical practice supports this: for example, atezolizumab, nivolumab, pembrolizumab, rucaparib, niraparib, olaparib, and ixazomib, some of which are first-line therapies, all have an ICER above $200,000, with a maximum ICER of $415,950 for nivolumab.[54] Therefore, CLAUDIA may be cost effective compared to TDM depending on society's willingness to pay. Moreover, our model found CLAUDIA to be cost effective compared to the current standard of care, BSA-based dosing, demonstrating that CLAUDIA may be able to provide a cost-effective improvement in treatment to patients. Our sensitivity analysis, which explored the effect of changes in the parameters used in our model, found that for all ranges tested, the ICER of CLAUDIA compared to BSA remained under $140,000/QALY (Data S1 Figure 4A), which is below the ICER of other interventions for patients with cancer treated clinically.

The AUC for 5-FU has been used in the literature to determine the optimal concentration of 5-FU for superior outcomes.[18] Often, the AUC is estimated based upon a small number of time points, which does not take the circadian effects on drug concentration into effect, and thus these AUC estimates may be inaccurate due to how the concentration of 5-FU can vary up to 8-fold for a given patient over the course of a single constant rate infusion.[7] CLAUDIA could enable the full concentration-time profile of 5-FU to be measured, which could lead clinicians to determine superior correlations and metrics to use to correlate concentration-time data for a drug to clinical outcomes. Thus, CLAUDIA could enable the true optimal concentration, or true optimal concentration-time profile, to be determined and used for administering 5-FU to patients.

Limitations of study

There are multiple aspects of future work that are needed to address the limitations of this study before CLAUDIA can reach the clinic. First, we performed the different steps in the closed-loop process for CLAUDIA manually, and future work will focus on using commercially available devices to automate all steps of the process (Figure S1D). Specifically, we could use Agilent's AssayMap Bravo system, which is an automated liquid handler, to perform the sample preparation steps of the human

blood. The Bravo system could use a Captiva EMR-lipid filtration plate for the filtration step. After the sample is processed in this manner, the samples would be ready to be loaded onto the HPLC-MS, which directly integrates with the Bravo system. The HPLC-MS system would be controlled by Agilent OpenLab CDS Online LC Monitoring Software, which both controls the HPLC-MS and enables near-real-time data analysis automatically. The concentration would then be automatically input into the control algorithm that could be implemented in the OpenLab Online software, which would then change the infusion rate of a syringe pump controlled by the software. Likewise, OpenLab could control a peristaltic pump to draw blood from the patient every 4 min. Next, although HPLC-MS has multiple benefits that make it an ideal sensor for CLAUDIA, one drawback of current HPLC-MS systems is that they are not portable. Thus, currently, CLAUDIA would be limited to inpatient use, which could still be beneficial in multiple clinical scenarios. Moreover, multiple companies are currently working on developing miniaturized MS, and further efforts in this field could enable CLAUDIA to become a portable system.[55] Importantly, future translation of CLAUDIA will involve delineation of clinical endpoints with respect to safety and efficacy benefits of CLAUDIA over the current standard of care, as current clinical trial data are informed by weight- and height-based dosing measures (including BSA-based dosing) as opposed to strictly controlled systemic chemotherapeutic levels.

Conclusion

CLAUDIA can control the concentration-time profile of 5-FU under a range of clinically relevant scenarios, and its use of commercially available components may allow the path to the clinic to be rapid. We demonstrated that CLAUDIA outperforms BSA-based dosing at maintaining the concentration of 5-FU within the target range under a variety of different rabbit PK profiles that resembles the PK variability of 5-FU observed clinically. CLAUDIA may thus increase the efficacy while decreasing the toxicity of chemotherapy, as multiple studies have demonstrated that individualizing the dose of 5-FU to patients results in superior clinical outcomes.[18,19,51] 5-FU is only one example of a drug that experiences significant PK variability in the clinic; we demonstrate that CLAUDIA is capable of detecting multiple additional chemotherapies simultaneously, and thus further studies should be performed to investigate CLAUDIA's performance in controlling the concentration-time profile of those drugs. Moreover, our CUA demonstrates that CLAUDIA is cost effective compared to the current standard of care for dosing 5-FU (i.e., BSA-based dosing). Overall, our results support the further development of CLAUDIA toward clinical translation, as it can control the concentration-time profile of 5-FU and may thereby improve the safety and efficacy of 5-FU for many patients.

STAR★METHODS

Detailed methods are provided in the online version of this paper and include the following:

- KEY RESOURCES TABLE
- RESOURCE AVAILABILITY
  - Lead contact
  - Materials availability
  - Data and code availability
- EXPERIMENTAL MODEL AND STUDY PARTICIPANT DETAILS
  - Study design
- METHOD DETAILS
  - HPLC-MS method development for 5-FU
  - Controller design

SUPPLEMENTAL INFORMATION

Supplemental information can be found online at https://doi.org/10.1016/j.medj.2024.03.020.

ACKNOWLEDGMENTS

Original artwork and illustrations were done by V.E. Fulford, Alar Illustration. We thank James Byrne, Seokkee Min, Sean You, Tom Kerssemakers, Kait Hess-Jimenez, Avik Som, Joy Collins, Jan-Georg Rosenboom, Gary Liu, Matt Murphy, Troy Kang, Benjamin Muller, and Joshua Bernstock from the Langer and Traverso Labs for helpful conversations regarding the project. We thank Jia Liang, Parmiss Khosravi, and Nhi Phan for help with ordering the materials used in this project. We thank Fenton Woods Laboratories for the use of the LC-TOF instrument used in these studies and for the support and guidance in preclinical analysis. We thank Trevor Carter for the use of the camera for the pictures in Figures S1A–S1C. Figure 1 was created with BioRender.com. We thank our funding sources, including the National Science Foundation Graduate Research Fellowship Program under grant no. 1745302, a MathWorks Fellowship (L.B.D.), MIT's Karl van Tassel (1925) Career Development Professorship and Department of Mechanical Engineering (G.T.), and the Bridge Project, a partnership between the Koch Institute for Integrative Cancer Research at MIT and the Dana-Farber/Harvard Cancer Center (L.B.D., G.T., R.L.).

AUTHOR CONTRIBUTIONS

Conceptualization, L.B.D., A.L., C.M.C., R.L., and G.T.; analytical chemistry experiments, L.B.D., K.A.H., A.L., N. Fitzgerald, E.M., J.M., and N.Z.; *in vivo* experiments, L.B.D., K.A.H., J.J., N. Fitzgerald, E.M., N. Fabian, W.M., K.I., J.L.P.K., and A.M.H.; designed control algorithm, L.B.D., H.-W.H., and D.T.; performed PK modeling, L.B.D., A.R.K., and D.T.; cost-effectiveness analysis, L.B.D., J.N.C., and T.Q.; formulation of DPD inhibitor for *in vivo* experiments, L.B.D., K.A.H., A.R.K., and M.C.; clinical perspective on the use of CLAUDIA, B.M.W., D.A.R., and G.T.; funding and supervision, L.B.D., R.L., and G.T.; analyzed and presented the data, L.B.D., K.A.H., A.L., N. Fitzgerald, E.M., J.M., J.N.C., N.B.L., and S.S.S.; unrestricted access to data, L.B.D., K.A.H., A.L., J.J., N. Fitzgerald, N. Fabian, J.M., A.R.K., A.M.H., R.L., and G.T.; writing – original draft, L.B.D. and K.A.H.; writing – review & editing, all authors approved the final article and take responsibility for its content.

DECLARATION OF INTERESTS

L.B.D., A.L., R.L., and G.T. have a provisional patent regarding this work. C.M.C. is an employee at Agilent Technologies. B.M.W. has received institutional research support from Celgene, Eli Lilly, Novartis, and Revolution Medicines; B.M.W. also consults for Celgene, GRAIL, and Mirati Therapeutics outside the described work. D.A.R. is an advisor for Axial Therapeutics (2022–present). He has consulted for Augmenix (2017–2019), Boston Scientific (2020–2021), Instylla (2022–present), Taiho (2023), and SirTex (2023). Complete details for R.L. can be found at the following

link: https://www.dropbox.com/s/yc3xqb5s8s94v7x/Rev%20Langer%20COI.pdf?dl=0. Complete details of all relationships for profit and not for profit for G.T. can be found at the following link. https://www.dropbox.com/sh/szi7vnr4a2ajb56/AABs5N5i0q9AfT1IqIJAE-T5a?dl=0.

Received: October 27, 2023
Revised: January 26, 2024
Accepted: March 21, 2024
Published: April 24, 2024

REFERENCES

1. Lee, J.J., Beumer, J.H., and Chu, E. (2016). Therapeutic drug monitoring of 5-fluorouracil. Cancer Chemother. Pharmacol. *78*, 447–464. https://doi.org/10.1007/s00280-016-3054-2.

2. Cespedes Feliciano, E.M., Chen, W.Y., Lee, V., Albers, K.B., Prado, C.M., Alexeeff, S., Xiao, J., Shachar, S.S., and Caan, B.J. (2019). Body Composition, Adherence to Anthracycline and Taxane-Based Chemotherapy, and Survival After Nonmetastatic Breast Cancer. JAMA Oncol.

3. Kline, C.L.B., Schiccitano, A., Zhu, J., Beachler, C., Sheikh, H., Harvey, H.A., Mackley, H.B., McKenna, K., Staveley-O'Carroll, K., Poritz, L., et al. (2014). Personalized dosing via pharmacokinetic monitoring of 5-fluorouracil might reduce toxicity in early- or late-stage colorectal cancer patients treated with infusional 5-fluorouracil-based chemotherapy regimens. Clin. Colorectal Cancer *13*, 119–126. https://doi.org/10.1016/j.clcc.2013.11.001.

4. White, J., Hu, P., Bonen, M., Bamat, M.K., and von Borstel, R. (2011). Point-of-care (POC) diagnostic assay for 5-fluorouracil (5-FU) quantitation to enable dose adjustment and detect dihydropyrimidine dehydrogenase (DPD) deficiency. J. Clin. Oncol. *29*, e19562. https://doi.org/10.1200/jco.2011.29.15_suppl.e19562.

5. Du BOIS, D., and Du BOIS, E.F. (1916). Clinical Calorimetry: Tenth Paper. A formula to estimate the approximate surface area if height and weight be known. Arch. Intern. Med. *XVII*, 863–871. https://doi.org/10.1001/archinte.1916.00080130010002.

6. DeRidder, L., Rubinson, D.A., Langer, R., and Traverso, G. (2022). The past, present, and future of chemotherapy with a focus on individualization of drug dosing. J. Controlled Release *352*, 840–860. https://doi.org/10.1016/j.jconrel.2022.10.043.

7. Metzger, G., Massari, C., Etienne, M.-C., Comisso, M., Brienza, S., Touitou, Y., Milano, G., Bastian, G., Misset, J.L., and Lévi, F. (1994). Spontaneous or imposed circadian changes in plasma concentrations of 5-fluorouracil coadministered with folinic acid and oxaliplatin: Relationship with mucosal toxicity in patients with cancer. Clin. Pharmacol. Ther. *56*, 190–201. https://doi.org/10.1038/clpt.1994.123.

8. Mosteller, R.D. (1987). Simplified Calculation of Body-Surface Area. N. Engl. J. Med. *317*, 1098. https://doi.org/10.1056/NEJM198710223171717.

9. Reyner, E., Lum, B., Jing, J., Kagedal, M., Ware, J.A., and Dickmann, L.J. (2020). Intrinsic and Extrinsic Pharmacokinetic Variability of Small Molecule Targeted Cancer Therapy. Clin. Transl. Sci. *13*, 410–418. https://doi.org/10.1111/cts.12726.

10. Hitchings, R., and Kelly, L. (2019). Predicting and Understanding the Human Microbiome's Impact on Pharmacology. Trends Pharmacol. Sci. *40*, 495–505. https://doi.org/10.1016/j.tips.2019.04.014.

11. Koppel, N., Rekdal, V.M., and Balskus, E.P. (2017). Chemical transformation of xenobiotics by the human gut microbiota. Science *356*. https://doi.org/10.1126/science.aag2770.

12. Zhang, J., Zhang, J., and Wang, R. (2018). Gut microbiota modulates drug pharmacokinetics. Drug Metab. Rev. *50*, 357–368. https://doi.org/10.1080/03602532.2018.1497647.

13. Schmetzer, O., and Flörcken, A. (2012). Sex Differences in the Drug Therapy for Oncologic Diseases. In Sex and Gender Differences in Pharmacology Handbook of Experimental Pharmacology, V. Regitz-Zagrosek, ed. (Springer), pp. 411–442. https://doi.org/10.1007/978-3-642-30726-3_19.

14. Ruben, M.D., Smith, D.F., FitzGerald, G.A., and Hogenesch, J.B. (2019). Dosing time matters. Science *365*, 547–549. https://doi.org/10.1126/science.aax7621.

15. Phan, V.H., Moore, M.M., McLachlan, A.J., Piquette-Miller, M., Xu, H., and Clarke, S.J. (2009). Ethnic differences in drug metabolism and toxicity from chemotherapy. Expert Opin. Drug Metab. Toxicol. *5*, 243–257. https://doi.org/10.1517/17425250902800153.

16. Beumer, J.H., Boisdron-Celle, M., Clarke, W., Courtney, J.B., Egorin, M.J., Gamelin, E., Harney, R.L., Hammett-Stabler, C., Lepp, S., Li, Y., et al. (2009). Multicenter evaluation of a novel nanoparticle immunoassay for 5-fluorouracil on the Olympus AU400 analyzer. Ther. Drug Monit. *31*, 688–694. https://doi.org/10.1519/JSC.0b013e3181b866d0.

17. Büchel, B., Sistonen, J., Joerger, M., Aebi, Y., Schürch, S., and Largiadèr, C.R. (2013). Comparative evaluation of the My5-FU™ immunoassay and LC-MS/MS in monitoring the 5-fluorouracil plasma levels in cancer patients. Clin. Chem. Lab. Med. *51*, 1681–1688. https://doi.org/10.1515/cclm-2012-0641.

18. Gamelin, E., Delva, R., Jacob, J., Merrouche, Y., Raoul, J.L., Pezet, D., Dorval, E., Piot, G., Morel, A., and Boisdron-Celle, M. (2008). Individual fluorouracil dose adjustment based on pharmacokinetic follow-up compared with conventional dosage: results of a multicenter randomized trial of patients with metastatic colorectal cancer. J. Clin. Oncol. Off. J. Am. Soc. Clin. Oncol. *26*, 2099–2105. https://doi.org/10.1200/JCO.2007.13.3934.

19. Capitain, O., Asevoaia, A., Boisdron-Celle, M., Poirier, A.-L., Morel, A., and Gamelin, E. (2012). Individual fluorouracil dose adjustment in FOLFOX based on pharmacokinetic follow-up compared with conventional body-area-surface dosing: a phase II, proof-of-concept study. Clin. Colorectal Cancer *11*, 263–267. https://doi.org/10.1016/j.clcc.2012.05.004.

20. Messori, M., Paolo Incremona, G., Cobelli, C., and Magni, L. (2018). Individualized model predictive control for the artificial pancreas: In silico evaluation of closed-loop glucose control. IEEE Control Syst. Mag. *38*, 86–104. https://doi.org/10.1109/MCS.2017.2766314.

21. Commissioner, O. of the (2020). FDA Authorizes First Interoperable, Automated Insulin Dosing Controller Designed to Allow More Choices for Patients Looking to Customize Their Individual Diabetes Management Device System (FDA). http://www.fda.gov/news-events/press-announcements/fda-authorizes-first-interoperable-automated-insulin-dosing-controller-designed-allow-more-choices.

22. Brown, S.A., Kovatchev, B.P., Raghinaru, D., Lum, J.W., Buckingham, B.A., Kudva, Y.C., Laffel, L.M., Levy, C.J., Pinsker, J.E., Wadwa, R.P., et al. (2019). Six-Month Randomized, Multicenter Trial of Closed-Loop Control in Type 1 Diabetes. N. Engl. J. Med. *381*, 1707–1717. https://doi.org/10.1056/NEJMoa1907863.

23. Cobelli, C., Renard, E., and Kovatchev, B. (2011). Artificial Pancreas: Past, Present, Future. Diabetes *60*, 2672–2682. https://doi.org/10.2337/db11-0654.

24. Kovatchev, B. (2019). A Century of Diabetes Technology: Signals, Models, and Artificial Pancreas Control. Trends Endocrinol. Metab. *30*, 432–444. https://doi.org/10.1016/j.tem.2019.04.008.

25. Mage, P.L., Ferguson, B.S., Maliniak, D., Ploense, K.L., Kippin, T.E., and Soh, H.T. (2017). Closed-loop control of circulating drug levels in live animals. Nat. Biomed. Eng. *1*, 1–10. https://doi.org/10.1038/s41551-017-0070.

26. Harris, D. (2010). Quantitative Chemical Analysis, 8th Edition (W.H. Freeman & Company).

27. Shiraiwa, K., Suzuki, Y., Uchida, H., Iwashita, Y., Tanaka, R., Iwao, M., Tada, K., Hirashita, T., Masuda, T., Endo, Y., et al. (2021). Simultaneous quantification method for 5-FU, uracil, and tegafur using UPLC-MS/MS and clinical application in monitoring UFT/LV combination therapy after hepatectomy. Sci. Rep. *11*, 3132. https://doi.org/10.1038/s41598-021-82908-8.

28. Arroyo-Currás, N., Ortega, G., Copp, D.A., Ploense, K.L., Plaxco, Z.A., Kippin, T.E., Hespanha, J.P., and Plaxco, K.W. (2018). High-Precision Control of Plasma Drug Levels Using Feedback-Controlled Dosing. ACS Pharmacol. Transl. Sci. *1*, 110–118. https://doi.org/10.1021/acsptsci.8b00033.

29. Furlong, M.T., Savant, I., Yuan, M., Scott, L., Mylott, W., Mariannino, T., Kadiyala, P., Roongta, V., and Arnold, M.E. (2013). A validated HPLC–MS/MS assay for quantifying unstable pharmacologically active metabolites of clopidogrel in human plasma: Application to a clinical pharmacokinetic study. J. Chromatogr. B *926*, 36–41. https://doi.org/10.1016/j.jchromb.2013.02.031.

30. Fang, L., Jiang, Y., Yang, Y., Zheng, Y., Zheng, J., Jiang, H., Zhang, S., Lin, L., Zheng, J., Zhang, S., et al. (2016). Determining the optimal 5-FU therapeutic dosage in the treatment of colorectal cancer patients. Oncotarget *7*, 81880–81887. https://doi.org/10.18632/oncotarget.11980.

31. Joshi, S.S., Catenacci, D.V.T., Karrison, T.G., Peterson, J.D., Zalupski, M.M., Sehdev, A., Wade, J., Sadiq, A., Picozzi, V.J., Amico, A., et al. (2020). Clinical Assessment of 5-Fluorouracil/Leucovorin, Nab-Paclitaxel, and Irinotecan (FOLFIRABRAX) in Untreated Patients with Gastrointestinal Cancer Using UGT1A1 Genotype–Guided Dosing. Clin. Cancer Res. *26*, 18–24. https://doi.org/10.1158/1078-0432.CCR-19-1483.

32. Boland, P.M., and Hochster, H.S. (2020). Making Fluorouracil "Sexy" Again. JNCI J. Natl. Cancer Inst. https://doi.org/10.1093/jnci/djaa125.

33. Jacobs, B.A.W., Deenen, M.J., Pluim, D., Hasselt, J.G.C. van, Krähenbühl, M.D., Geel, R.M.J.M. van, Vries, N. de, Rosing, H., Meulendijks, D., Burylo, A.M., et al. (2016). Pronounced between-subject and circadian variability in thymidylate synthase and dihydropyrimidine dehydrogenase enzyme activity in human volunteers. Br. J. Clin. Pharmacol. *82*, 706–716. https://doi.org/10.1111/bcp.13007.

34. Harris, B.E., Song, R., Soong, S.J., and Diasio, R.B. (1990). Relationship between dihydropyrimidine dehydrogenase activity and plasma 5-fluorouracil levels with evidence for circadian variation of enzyme activity and plasma drug levels in cancer patients receiving 5-fluorouracil by protracted continuous infusion. Cancer Res. *50*, 197–201.

35. Longley, D.B., Harkin, D.P., and Johnston, P.G. (2003). 5-Fluorouracil: mechanisms of action and clinical strategies. Nat. Rev. Cancer *3*, 330–338. https://doi.org/10.1038/nrc1074.

36. Amstutz, U., Froehlich, T.K., and Largiadèr, C.R. (2011). Dihydropyrimidine dehydrogenase gene as a major predictor of severe 5-fluorouracil toxicity. Pharmacogenomics *12*, 1321–1336. https://doi.org/10.2217/pgs.11.72.

37. Diasio, R.B., and Harris, B.E. (1989). Clinical pharmacology of 5-fluorouracil. Clin. Pharmacokinet. *16*, 215–237. https://doi.org/10.2165/00003088-198916040-00002.

38. Zurayk, M., Keung, Y.-K., Yu, D., and Hu, E.H. (2019). Successful use of uridine triacetate (Vistogard) three weeks after capecitabine in a patient with homozygous dihydropyrimidine dehydrogenase mutation: A case report and review of the literature. J. Oncol. Pharm. Pract. *25*, 234–238. https://doi.org/10.1177/1078155217732141.

39. Gamelin, E., Boisdron-celle, M., Delva, R., Lortholary, A., Genevieve, F., Larra, F., Ifrah, N., and Robert, J. (1999). Correlation Between Uracil and Dihydrouracil Plasma Ratio, Fluorouracil (5-FU) Pharmacokinetic Parameters, and Tolerance in Patients With Advanced Colorectal Cancer: A Potential Interest for Predicting 5-FU Toxicity and Determining Optimal 5-FU Dosage. J. Clin. Oncol. https://doi.org/10.1200/jco.1999.17.4.1105.

40. Thyss, A., Milano, G., Renée, N., Vallicioni, J., Schneider, M., and Demard, F. (1986). Clinical pharmacokinetic study of 5-FU in continuous 5-day infusions for head and neck cancer. Cancer Chemother. Pharmacol. *16*, 64–66. https://doi.org/10.1007/BF00255288.

41. Schmoll, H.-J. (2003). Dihydropyrimidine dehydrogenase inhibition as a strategy for the oral administration of 5-fluorouracil: utility in the treatment of advanced colorectal cancer. Anti Cancer Drugs *14*, 695–702. https://doi.org/10.1097/00001813-200310000-00003.

42. Nishiyama, T., Ogura, K., Okuda, H., Suda, K., Kato, A., and Watabe, T. (2000). Mechanism-based inactivation of human dihydropyrimidine dehydrogenase by (E)-5-(2-bromovinyl)uracil in the presence of NADPH. Mol. Pharmacol. *57*, 899–905.

43. Saif, M.W., and Diasio, R.B. (2016). Benefit of uridine triacetate (Vistogard) in rescuing severe 5-fluorouracil toxicity in patients with dihydropyrimidine dehydrogenase (DPYD) deficiency. Cancer Chemother. Pharmacol. *78*, 151–156. https://doi.org/10.1007/s00280-016-3063-1.

44. O'Malley, P.A. (2016). Vistogard (Uridine Triacetate): The First and Only Drug Approved for the Treatment of 5-Fluorouracil or Capecitabine Overdose: Implications for the Clinical Nurse Specialist. Clin. Nurse Spec. *30*, 145–147. https://doi.org/10.1097/NUR.0000000000000198.

45. Milano, G., Roman, P., Khater, R., Frenay, M., Renee, N., and Namer, M. (1988). Dose Versus pharmacokinetics for predicting tolerance to 5-day continuous infusion of 5-FU. Int. J. Cancer *41*, 537–541. https://doi.org/10.1002/ijc.2910410411.

46. Seborg, D., Edgar, T., Mellichamp, D., and Doyle III, F. (2011). Process Dynamics and Control, Third Edition (Wiley).

47. Center for Drug Evaluation and Research (2020). Bioanalytical Method Validation Guidance for Industry. US Food Drug Adm. https://www.fda.gov/regulatory-information/search-fda-guidance-documents/bioanalytical-method-validation-guidance-industry.

48. Chen, D., Cheng, J., Yang, K., Ma, Y., and Yang, F. (2013). Retrospective analysis of chronomodulated chemotherapy versus conventional chemotherapy with paclitaxel, carboplatin, and 5-fluorouracil in patients with recurrent and/or metastatic head and neck squamous cell carcinoma. OncoTargets Ther. *6*, 1507–1514. https://doi.org/10.2147/OTT.S53098.

49. Lévi, F.A., Zidani, R., Vannetzel, J.-M., Perpoint, B., Focan, C., Faggiuolo, R., Chollet, P., Garufi, C., Itzhaki, M., Dogliotti, L., et al. (1994). Chronomodulated Versus Fixed-Infusion—Rate Delivery of Ambulatory Chemotherapy With Oxaliplatin, Fluorouracil, and Folinic Acid (Leucovorin) in Patients With Colorectal Cancer Metastases: a Randomized Multi-institutional Trial. JNCI J. Natl. Cancer Inst. *86*, 1608–1617. https://doi.org/10.1093/jnci/86.21.1608.

50. Lévi, F., Zidani, R., and Misset, J.L. (1997). Randomised multicentre trial of chronotherapy with oxaliplatin, fluorouracil, and folinic acid in metastatic colorectal cancer. International Organization for Cancer Chronotherapy. Lancet Lond. Engl. *350*, 681–686. https://doi.org/10.1016/s0140-6736(97)03358-8.

51. Clarke, W.A., Chatelut, E., Fotoohi, A.K., Larson, R.A., Martin, J.H., Mathijssen, R.H.J., and Salamone, S.J. (2021). Therapeutic drug monitoring in oncology: International Association of Therapeutic Drug Monitoring and Clinical Toxicology consensus guidelines for imatinib therapy. Eur. J. Cancer *157*, 428–440. https://doi.org/10.1016/j.ejca.2021.08.033.

52. Palma, L.B., Coito, F.V., and Gil, P.S. (2011). Real-time detection of oscillations in control loops. In 2011 International Conference on Power Engineering, Energy and Electrical Drives, pp. 1–6. https://doi.org/10.1109/PowerEng.2011.6036424.

53. Neumann, P.J., and Kim, D.D. (2023). Cost-effectiveness Thresholds Used by Study Authors, 1990-2021. JAMA *329*, 1312–1314. https://doi.org/10.1001/jama.2023.1792.

54. Cherla, A., Renwick, M., Jha, A., and Mossialos, E. (2020). Cost-effectiveness of cancer drugs: Comparative analysis of the United States and England. EClinicalMedicine *29*. https://doi.org/10.1016/j.eclinm.2020.100625.

55. Mielczarek, P., Silberring, J., and Smoluch, M. (2020). Miniaturization in Mass Spectrometry. Mass Spectrom. Rev. *39*, 453–470. https://doi.org/10.1002/mas.21614.

56. Discrete-time PID Controller Implementation | ESI Group (2015). https://www.scilab.org/discrete-time-pid-controller-implementation.

57. Tsibiribi, P., Bui-Xuan, C., Bui-Xuan, B., Lombard-Bohas, C., Duperret, S., Belkhiria, M., Tabib, A., Maujean, G., Descotes, J., and Timour, Q. (2006). Cardiac lesions induced by 5-fluorouracil in the rabbit. Hum. Exp. Toxicol.

25, 305–309. https://doi.org/10.1191/0960327106ht628oa.

58. Cwikiel, M., Eskilsson, J., Wieslander, J., Stjernquist, U., and Albertsson, M. (1996). The Appearance of Endothelium in Small Arteries After Treatment with 5-Fluorouracil. An Electron Microscopic Study of Late Effects in Rabbits. Scanning Microsc. *10*.

59. Sara, J.D., Kaur, J., Khodadadi, R., Rehman, M., Lobo, R., Chakrabarti, S., Herrmann, J., Lerman, A., and Grothey, A. (2018). 5-fluorouracil and cardiotoxicity: a review. Ther. Adv. Med. Oncol. *10*. https://doi.org/10.1177/1758835918780140.

60. Itoh, T., Kawabe, M., Nagase, T., Koike, T., Miyoshi, M., and Miyahara, K. (2018). Measurements of body surface area and volume in laboratory rabbits (New Zealand White rabbits) using a computed tomography scanner. Exp. Anim. *67*, 527–534. https://doi.org/10.1538/expanim.18-0028.

61. Neumann, P.J., Cohen, J.T., and Weinstein, M.C. (2014). Updating cost-effectiveness–the curious resilience of the $50,000-per-QALY threshold. N. Engl. J. Med. *371*, 796–797. https://doi.org/10.1056/NEJMp1405158.

62. Sanders, G.D., Neumann, P.J., Basu, A., Brock, D.W., Feeny, D., Krahn, M., Kuntz, K.M., Meltzer, D.O., Owens, D.K., Prosser, L.A., et al. (2016). Recommendations for Conduct, Methodological Practices, and Reporting of Cost-effectiveness Analyses: Second Panel on Cost-Effectiveness in Health and Medicine. JAMA *316*, 1093–1103. https://doi.org/10.1001/jama.2016.12195.

63. Schmoll, H.-J., Cunningham, D., Sobrero, A., Karapetis, C.S., Rougier, P., Koski, S.L., Kocakova, I., Bondarenko, I., Bodoky, G., Mainwaring, P., et al. (2012). Cediranib with mFOLFOX6 versus bevacizumab with mFOLFOX6 as first-line treatment for patients with advanced colorectal cancer: a double-blind, randomized phase III study (HORIZON III). J. Clin. Oncol. Off. J. Am. Soc. Clin. Oncol. *30*, 3588–3595. https://doi.org/10.1200/JCO.2012.42.5355.

64. Consumer Price Index: U.S. Bureau of Labor Statistics https://www.bls.gov/cpi/.

65. Arias, E., and Xu, J.; United States CDC United States Life Tables (2015)67 (National Vital Statistics Reports), Number 7.

66. Yamazaki, K., Nagase, M., Tamagawa, H., Ueda, S., Tamura, T., Murata, K., Eguchi Nakajima, T., Baba, E., Tsuda, M., Moriwaki, T., et al. (2016). Randomized phase III study of bevacizumab plus FOLFIRI and bevacizumab plus mFOLFOX6 as first-line treatment for patients with metastatic colorectal cancer (WJOG4407G). Ann. Oncol. Off. J. Eur. Soc. Med. Oncol. *27*, 1539–1546. https://doi.org/10.1093/annonc/mdw206.

67. Venook, A.P., Niedzwiecki, D., Lenz, H.-J., Innocenti, F., Fruth, B., Meyerhardt, J.A., Schrag, D., Greene, C., O'Neil, B.H., Atkins, J.N., et al. (2017). Effect of First-Line Chemotherapy Combined With Cetuximab or Bevacizumab on Overall Survival in Patients With KRAS Wild-Type Advanced or Metastatic Colorectal Cancer: A Randomized Clinical Trial. JAMA *317*, 2392–2401. https://doi.org/10.1001/jama.2017.7105.

STAR★METHODS

KEY RESOURCES TABLE

REAGENT or RESOURCE	SOURCE	IDENTIFIER
Biological samples		
Defibrinated Rabbit Blood	Rockland Immunochemicals	Cat#R109-0100; CAS: N/A
Chemicals, peptides, and recombinant proteins		
Fluorouracil Injection, USP	McKesson (Produced by Accord Healthcare)	Cat# 999137; NDC#: 16729-276-68
5-fluorouracil (≥99%, powder)	Sigma-Aldrich	Cat#F6627; CAS: 51-21-8
(E)-5-(2-bromovinyl) uracil (97%, powder)	Sigma-Aldrich	Cat#457442; CAS: 69304-49-0
5-bromouracil (98%, powder)	Sigma-Aldrich	Cat#852473; CAS: 200-084-0
Irinotecan hydrochloride (≥97%, powder)	Sigma-Aldrich	Cat#I1406; CAS: 100286-90-6
Theophylline (≥99%, powder)	Sigma-Aldrich	Cat#T1633-50G; CAS: 58-55-9
Thiotepa (United States Pharmacopeia (USP) reference standard)	United States Pharmacopeia	Cat#1664000; CAS: 52-24-4
Doxorubicin hydrochloride (certified reference material, powder)	Sigma-Aldrich	Cat#PHR1789-200MG; CAS: 25316-40-9
Cyclophosphamide (certified reference material, powder)	Sigma-Aldrich	Cat#PHR1404-1G; CAS: 6055-19-2
8-chlorotheophylline (USP reference standard, powder)	Sigma-Aldrich	Cat#1121038-200MG; CAS: 85-18-7
Kollisolv® PEG E 300	Sigma-Aldrich	Cat#91462; CAS: 25322-68-3
TWEEN® 80 (Polysorbate 80)	Sigma-Aldrich (SAFC Commercial)	Cat#8.17061.2500; CAS: 9005-65-6
DMSO, anhydrous	Invitrogen	Cat#D12345; CAS: 67-68-5
Sterile Water (USP 100%)	Aspen Veterinary Resources, LTD	Cat#15114151; NDC#: 46066-808-25
Sterile Saline Solution (0.9 g/100 mL)	Aspen Veterinary Resources, LTD	Cat#14208186; NDC#: 46066-807-25
0.9% Sodium Chloride Injection USP diluent	McKesson (Produced by Hospira, Inc.)	Cat#2718500; NDC#: 00409-4888-50
Dextrose Solution (50% w/v)	Aspen Veterinary Resources, LTD	Cat#15784324; NDC#: 46066-801-50
Acetonitrile (Optima, LC/MS Grade)	Fisher Scientific	Cat#A955-4; CAS: 75-05-8
Methanol (Optima, LC/MS Grade)	Fisher Scientific	Cat#A456-4; CAS: 67-56-1
Deposited data		
See Mendeley data and code upload for this paper	This paper	https://doi.org/10.17632/jgf6m7x8nb.1
Experimental models: Organisms/strains		
New Zealand White Rabbits	Charles River Laboratories	Crl:KBL(NZW)
Software and algorithms		
PID control algorithm; SIMULINK model of system for controller development; data analysis code; TreeAge cost-effectiveness modeling software	This paper; Mendeley Data	https://doi.org/10.17632/jgf6m7x8nb.1
Other		
Mini Centrifuge (6,000 rpm, 2000xg)	Crystal Industries	Cat#MLX-106
Pump 33 DDS (Dual Drive System) Syringe Pump	Harvard Apparatus	Cat#70-3333

RESOURCE AVAILABILITY

Lead contact

Further information and requests for resources, data, and reagents should be directed to and will be fulfilled by the lead contact, Dr. Giovanni Traverso (cgt20@mit.edu).

Materials availability

This study did not generate any unique reagents.

Data and code availability

All original code and data have been deposited on Mendeley Data and is publicly available as of the date of publication according to a CC BY NC 3.0 license. https://doi.org/10.17632/jgf6m7x8nb.1.

EXPERIMENTAL MODEL AND STUDY PARTICIPANT DETAILS

Study design

We developed and validated a method to rapidly extract 5-FU from blood and analyze it on HPLC-MS. We determined the PK profile of 5-FU in rabbits given a continuous rate infusion (CRI)—both with and without a DPD inhibitor ((E)-5-(2-bromovinyl) uracil) to mimic the PK variability experienced clinically—to inform the design and tuning of a control algorithm. We evaluated the ability of CLAUDIA to bring the concentration of 5-FU to the target therapeutic window under basal conditions and in the presence of the DPD inhibitor; we also investigated CLAUDIA's ability to control 5-FU concentrations according to other concentration-time profiles. Lastly, we performed a cost-utility analysis to evaluate if CLAUDIA could be cost-effective in widespread clinical implementation.

METHOD DETAILS

HPLC-MS method development for 5-FU

Quantitation of 5-fluorouracil was achieved using an Agilent 1290 UHPLC system, consisting of a binary pump, autosampler, and temperature-controlled column compartment, coupled to a dual-nebulizer electrospray ionization (ESI) 'accurate mass' time-of-flight (TOF) mass spectrometer (Agilent Technologies, Santa Clara, CA). Whole-blood or plasma extracts were injected at a volume of 7.5 μL and separated isocratically on a SeQuant ZIC-HILIC column (50 × 4.6 mm, 3.5 μm, 200 Å) (Merck Millipore, Darmstadt, Germany) held at 40°C. The mobile phase consisted of 0.1% formic acid in water (v/v) (A), and acetonitrile (B), flowing at 0.6 mL/min at a composition of 80% B isocratically. ESI drying gas flowed at 10 L/min with a temperature of 350°C and nebulizer pressure of 40 psig. Spectra were obtained in negative ionization mode, with a fragmentor voltage of 80 V and capillary voltage of 4000 V, at a rate of 1 spectrum/s with a range of 100–1200 *m/z*. Accurate masses were corrected by bracketing reference mass ions at 112.9855 and 1033.9881 *m/z*.

Data processing of the output signal was performed using MassHunter Quantitative Analysis software (Version 10.1). Both 5-fluorouracil and 5-bromouracil eluted at 1.4 min. A retention time tolerance of ±0.5 min and an *m/z* tolerance of ±50 ppm was used for peak recognition. Calibration curves were generated by quantifying extracts of spiked blood at known concentration levels from 250 ng/mL to 60,000 ng/mL 5-fluorouracil and fitting with a 1/x-weighted linear regression. A 9-point calibration curve for 5-FU was run for each animal experiment on the day of the analysis.

Controller design

We used a PID controller with derivative filter.

$$C(s) = K_p + \frac{K_i}{s} + \frac{NK_d}{1+\frac{N}{s}}$$

We implemented the controller by using the backward Euler method, as previously derived.[56] To tune our controller, we first modeled our system as a first-order system, using the continuous rate infusion experiments to determine the gain and time constant of our system (Figures S3A and S3B). We then used SIMULINK (version

R2020b, 10.2) to simulate our system and tune our controller, using an adaptation of a SIMULINK model previously published.[25] We simulated both the 8-min time delay that is present in our system, and the 4-min sampling rate. We additionally added noise to our measurements to mimic the noise seen in concentration measurements with HPLC-MS. We then tuned our controller by first finding the values of K_P and K_I that would result in instability of the system in a proportional-only or integral-only system, respectively. We then reduced the values of both these controller gains by at least half, and then we tuned K_D and N empirically via simulations. We continued to alter the controller gains until we achieved an acceptable rise time (i.e., under 1 h) that resulted in a stable system under a range of system conditions (i.e., system gains and time constants) to mimic the widespread PK variability observed clinically. To prevent issues that may arise due to limitations associated with the infusion system (e.g., due to the pump leaking), as a safety measure we implemented a rule-based component of our controller. The rule was triggered if the concentration decreased by 50% or more, while the infusion rate increased for each of the past two timepoints. If this condition were to be met, then the infusion rate is kept constant, as the positive feedback loop could result in a runaway infusion rate. Clinically, when this rule is triggered, the system could also trigger an alarm to alert the patient's caregivers that there is a problem with the infusion system. We decided to use the gains: K_P: 0.2, K_I: 0.0003, K_D: 15, and N (derivative filter): 0.009. These controller gains allowed for sufficient control of 5-FU concentrations under a range of 5-FU PK models in the rabbits according to our simulations (Figure S3C). We implemented anti-windup in the controller by setting a maximum and minimum flow rate that could be used at any time. The minimum was set to 0 μL/s, while the maximum was set to 10 μL/s. We implemented the controller using Python.

In vivo experiments

Rabbits were anesthetized with intramuscular ketamine (35 mg/kg) and xylazine (5 mg/kg), and intubated using an endotracheal tube, and maintained on 1–3% isoflurane in 100% oxygen (1.5–2.5L/min) on a Bain non-rebreathing circuit. During anesthesia, the rabbits were monitored for heart rate, oxygen saturation (SpO_2), respiratory rate, end-tidal carbon dioxide ($EtCO_2$), and body temperature. Ophthalmic ointment was applied to both eyes to prevent corneal drying. Peripheral ear catheters were placed bilaterally in the auricular artery for blood collection and in the lateral marginal ear vein for drug and fluid administration. Rabbits received a maintenance rate (3-5 mL/kg/h) of lactated Ringer's solution intravenously (IV) and were kept on a circulating warm water blanket to maintain body temperature during the procedure. All rabbits used in CLAUDIA experiments were anesthetized in the same manner and intubated before receiving IV propofol (approximately 0.5–1.5 mg/kg) for additional sedation during brief transport (<10 min) from the animal facility to the laboratory space containing the CLAUDIA system. No transport was performed for the control experiments (i.e., control experiments that observed the PK of the rabbits during BSA-based dosing without CLAUDIA control of the concentration).

Due to the potential toxicity of 5-FU that is reported in the literature, the first two rabbits administered 5-FU were non-survival experiments and were submitted for post-mortem evaluation. Findings indicative of respiratory and cardiac toxicities consistent with previous reports[57–59] led us to perform all subsequent experiments as non-survival experiments. Following each experiment, rabbits were euthanized by IV injection of sodium pentobarbital (390 mg) and disposed of in accordance with MIT EHS requirements.

For experiments where a DPD-inhibitor was delivered, a 12 Fr red rubber catheter was passed down the oral cavity and esophagus into the stomach of rabbits under anesthesia, and any liquid gastric contents were aspirated and discarded. The DPD-inhibitor was then administered through the catheter and flushed through the catheter with 6mL of sterile water. All waste products and biological materials were treated as hazardous and were handled and disposed of in accordance with MIT Environmental Health and Safety (EHS) standards.

All animal experiments were performed in compliance with Animal Use Protocols approved by the Committee on Animal Care at the Massachusetts Institute of Technology (protocol number: 2207000397). New Zealand White rabbits (Charles River Breeding Laboratories, Canada; female, 2.6–5.6 kg) were chosen as the model to evaluate the pharmacokinetics of 5-FU and the performance of the experiments evaluating CLAUDIA. Female rabbits were chosen for their size and ideal total blood volume, allowing for frequent blood sampling over the experimental period. Standard husbandry practices included light cycle of 12 h light, 12 h of dark, *ad libitum* water, measured quantity of pellets (Laboratory Rabbit Diet high fiber 5326, LabDiet), timothy hay, fresh fruit and vegetables.

Bolus experiments

3 mg/kg of a 5 mg/mL 5-FU in saline with 5% dextrose was infused intravenously through a venous ear catheter to a rabbit over 1 min by a syringe pump (Harvard Apparatus Pump33DDS). Blood was sampled via arterial ear catheter manually every 2 min for the first 30 min, and then every 2.5 min thereafter for a total of 2-h. During the experiments where we gave the DPD inhibitor, we administered 8.5 mg/kg of the inhibitor orally 90 min before the start of the bolus. The DPD inhibitor was dissolved to 5 mg/mL in 3% DMSO, 50% Tween 80, and 47% PEG 300 before being diluted 1 in 3 with sterile water.

Continuous rate infusion experiments

93 mg/m^2/h of a 4 mg/mL 5-FU in saline with 5% dextrose was infused intravenously through a venous ear catheter to a rabbit continuously over 4 h by a syringe pump (Harvard Apparatus Pump33DDS) with the blood being sampled every 4 min manually from an arterial ear catheter. The infusion then was stopped, and blood was still sampled for another hour; every 2 min for the first 20 min and every 4 min for the next 40-min. The BSA of the rabbits were calculated from the following equation[60].

$$BSA\left[m^2\right] = 0.11 * BW[kg]^{2/3}$$

For CRI + DPD inhibitor experiments, 8.5 mg/kg of the inhibitor was given orally right before the start of the infusion of the drug (i.e., right before time 0 min), as described above, and blood was sampled every 4 min for the duration of the experiment.

CLAUDIA experiments

These experiments were performed identical to the CRI experiments, except that the infusion rate was adjusted according to the control algorithm. Every 4 min, blood was sampled, immediately processed using our rapid sample preparation method, analyzed on our rapid HPLC-MS method, the resulting concentration was input into our controller, which was used to adjust the infusion rate of 5-FU into the rabbits. In the disturbance experiments, we administered 8.5 mg/kg of the DPD inhibitor orally 0 min into the experiment. The total duration of the experiment was 4 h. Concentration data for the closed-loop groups is plotted as the time the blood was sampled from the rabbit (and not the time the measurement was made from the HPLC-MS, which was 8 min later).

Methods for HPLC-MS method validation for 5-FU

For the calibration curve, we made three separate stock solutions of 5-FU at 1 mg/mL concentration to make 3 independent calibration curves. Then, keeping all vials separate, we serially diluted each 1 mg/mL stock down to both 0.1 mg/mL and 0.01 mg/mL. We spiked 225 μL blood with the appropriate 5-FU stock solution, diluting with water as needed. For example, for the 60 ppm concentration, we pipetted 15 μL of the 1 mg/mL stock and 10 μL of water into the 225 μL of blood, which was mixed by pipetting up and down. The blood was centrifuged for 30 s and 50 μL of the resulting plasma was added to 300 μL of 25:75 methanol:acetonitrile with 5-BU (5 ppm). The mixture was vortexed and then centrifuged for 30 s. The supernatant was aspirated into a syringe and filtered through an FS Overmolded 13 mm syringe filter into an HPLC vial. For the QC samples, the same process was performed, using an independent fourth stock of 5-FU. The accuracy is demonstrated as the average of the accuracies, and the precision is the % CV of the accuracies. The limit of detection (LOD) was calculated by multiplying the standard deviation of the $N = 6$ QCs near the LOD (at 0.5 mg/L) by 3, and dividing by the slope of the calibration curve, as previously described.[26] The calibration curves used a 1/x weighting of the concentrations.

For the recovery experiments, we made three independent calibration curves of single blanks spiked with 5-FU, which served as the "100% recovery" samples that we compared our samples that were produced as normal (as stated above). To make the calibration curves we made three independent stock solutions of 5-FU as above. We then made a single blank, by processing blood that was not spiked with 5-FU as stated above. Briefly, 200 μL of blood was centrifuged for 30 s, and 50 μL of plasma was added to 300 μL of 25:75 methanol:acetonitrile with 5-BU (5ppm), which was vortexed, centrifuged for 30 s, and filtered. To 200 μL of filtrate we added the proper amount of 5-FU stock solution to make the concentration of 5-FU in the filtrate the target concentration. We repeated this to make the complete calibration curve. The concentration of the filtrate for the sample produced with the normal sample preparation method (i.e., spike blood with 5-FU and then process the samples using our sample preparation method) were determined compared to the 100% recovery calibration curve. The recovery was determined by dividing the calculated concentration of the sample to the ideal concentration. The analysis was performed using Agilent MassHunter Quantitative Analysis' software. Validation was guided by the FDA's guidance to industry.[47]

We additionally performed a partial validation of the more rapid, alternative sample preparation technique that we developed. Briefly, 200 μL blood was added to 600 μL of 25%/75% methanol/acetonitrile with 5 μg/mL 5-bromouracil. The mixture was vortexed for 5 s, centrifuged for 30 s, the supernatant was aspirated into a syringe and then filtered. An overview of this process is shown in Figure S1B. We performed the validation using this method using the same procedure as above. For the recovery experiments, we produced single blanks using this method with blood that was not spiked, and then spiked the filtrates with 5-FU as described above to serve at the "100% recovery" samples.

Method for the multiple chemotherapies HPLC-MS method and method validation

HPLC-MS method. Chemotherapeutic drugs were separated and quantified on an Agilent 1290 liquid chromatography system coupled to a 6224A time-of-flight mass spectrometer (TOF MS, Agilent Technologies, Santa Clara, CA, USA). Separations were performed on an Agilent Poroshell 120 SB-Aq column (2.1 × 50 mm, 1.9 μm d_p), held at 25°C, by injecting 5 μL of sample and eluting with a mobile phase of

0.1% formic acid in water (v/v, A) and acetonitrile (B) at a flow rate of 1 mL/min. The gradient program used was 0 min, 2% B; 0.5 min, 2% B; 3.5 min, 100% B. The dual electrospray ionization source used nitrogen gas at 350°C, 11 L/min, at a pressure of 40 psig. The capillary voltage was set to 3500 V and the fragmentor voltage to 150 V. Mass spectra were acquired from 100 to 3000 *m/z* at a rate of 2 Hz. ToF acquisition was made in the positive mode. A continuous flow of a reference mixture through the second source nebulizer was used to calibrate the mass axis at 121.0509 *m/z* and 922.0098 *m/z*.

Data processing of the output signal was performed using MassHunter Quantitative Analysis software (version 10.1). The following parameters were used in the analysis

	Retention time (minutes)	Retention time tolerance (±minutes)	m/z
Irinotecan hydrochloride	1.755	1.0	587.2830
Theophylline	1.286	1.0	181.0647
Thiotepa	1.505	0.5	190.0489
Doxorubucin hydrochloride	1.779	0.5	544.1740
Cyclophosphamide	1.724	1.0	261.0248

A 100-ppm m/z tolerance was used for all compounds. A 9-point calibration curve with 1/x-weighted linear regression was used to generate calibration curves by quantifying extracts of spiked blood at known concentration levels from 0.5 mg/L to 60 mg/L.

Method validation for the multiple chemotherapies. The method validation for the HPLC-MS that was designed to analyze multiple chemotherapies simultaneously was performed as was the case for 5-FU, except here the three independent stock solutions used for this analysis had the multiple different chemotherapies mixed together in each of three independent stock solutions of the drug mixtures. The calibration curves were created with these stock solutions, and the QCs used a fourth independent stock solution of the multiple chemotherapies mixed together. For the single chemotherapy QCs, we spiked blood with a single chemotherapy to identify if mixing the chemotherapies together impacted the results. 8-chlorotheophylline at 5 ppm in the extraction solvent served as the internal standard for all samples.

Cost-utility analysis (CUA)

A Markov model of previously untreated mCRC patients on FOLFOX6 was developed to compare the cost-effectiveness of the closed-loop system compared to traditional BSA dosing and TDM using TreeAge Pro Healthcare 2020. We followed a cohort of 62-year-old men and women for a lifetime time horizon. All patients started in the stable on FOLFOX6 state. They could remain stable, progress to second-line treatment with FOLFIRI, or die due to the cancer or background death (i.e., normal causes of death for a person at the given age) (Figure 4A). The patient could remain in the progressed state before death due to cancer or background death but could not return to the stable disease state. Patients could change states after each cycle of chemotherapy, and the cycle length was set to 2 weeks to simulate the time between treatments in mCRC patients receiving FOLFOX6. In our model we utilized a US healthcare perspective, with a willingness-to-pay threshold was set to $100,000.[61] All costs and QALYs were discounted by 3% annually.[62] Half-cycle correction was applied to all cycle costs and state utilities. The primary outcomes are the incremental cost to effectiveness ratio (ICER), incremental cost, and

incremental effectiveness. *Capitain* et al. was used for the TDM arm and *Schmoll* et al. was used for the BSA arm.[19,63] The cost per cycle of the BSA, TDM and CLAUDIA groups were estimated as described in detail below. Briefly, the BSA group included the costs of drugs, administrative costs, 3 h at the infusion center, and costs for taking the portable infusion pump home. The TDM group included the costs of the BSA group plus the cost of the TDM test, and 1 h of a nurse's assistance to perform the TDM. The CLAUDIA group included the costs of the BSA group plus the costs of CLAUDIA, which was estimated by adding the cost of disposable materials to the upfront cost of CLAUDIA discounted over the expected number of uses. The upfront cost of CLAUDIA was the cost of an HPLC, MS, automated sample preparation device, autosampler, controller, and infusion pump. Annual maintenance costs were likewise distributed to the expected number of uses in the given time frame. The costs of the progressed state with patients receiving FOLFIRI was ~$53 less than in the FOLFOX6 arm, due to the differences in drug costs. All costs were converted to 2019 US dollars using the US Consumer Price Index.[64] In estimating the efficacy of the CLAUDIA group, since CLAUDIA will essentially perform TDM at multiple timepoints instead of just taking a blood sample at a single timepoint, we assumed in our base case that CLAUDIA will better than TDM in terms of reducing toxicities and extending both PFS and OS. We estimated the relative risk (RR) of CLAUDIA compared to TDM to be 0.75, 0.75, and 0.85 for toxicities, PFS and OS, respectively, and performed a one-way sensitivity analysis on these parameters, as well as other parameters (Data S1 Figures 4 and 5).

Transition probabilities were estimated from literature values. Ideally one study comparing the impacts of BSA and TDM dosing with the FOLFOX6 regimen in mCRC patients would have been used. However, such a study does not exist, and we thus used two different studies for the BSA and TDM arms separately. *Capitain* et al. was a Phase II clinical trial studying the impact of TDM on FOLFOX6 treatment, and was used for the TDM arm of the model, but since they did not report Kaplan-Meir (KM) curves for the BSA arm, we used *Schmoll* et al. for the BSA arm, which was a Phase III randomized control clinical trial in mCRC patients, with one arm as a BSA based dosing of FOLFOX6.[19,63] We overlaid the KM curves for the raw data from the paper and the KM curves generated by the software to demonstrate the model can replicate the published data (Data S1. Figure 6). Additional limitations inherent to the study design include differences in study population, adjunctive use of bevacizumab, and dosing of 5-FU and leucovorin (the initial dose of 5-FU was 2500 mg/m^2 compared to 2400 mg/m^2 in the BSA arm and the dose of leucovorin was 200 mg/m^2 instead of 400 mg/m).[19,63] Whenever a patient received FOLFOX6 treatment, they could experience diarrhea, neutropenia, mucositis or fibromyalgia (i.e., the most common toxicities with FOLFOX6 treatment), which incurred disutilities and costs (see Table S3). The probability of non-cancer based deaths (i.e., background deaths) was determined using data from the CDC.[65]

We set the RR for OS between CLAUDIA compared to the TDM group to 0.85, as the RR of the rates of overall death between the BSA and TDM arms was 0.85.[19,63] The RR for the rates of progression was 0.25 between the BSA and TDM arms; we decided to set the PFS RR between CLAUDIA and TDM arms to 0.75.[19,63] The RR for toxicities between CLAUDIA and TDM arms was assumed to be 0.75 in the base case, as there was a 95%, 86%, and 28% reduction in mucositis, diarrhea, and neutropenia, respectively, observed between the BSA and PK arms in *Capitain* et al.[19] We assumed the majority of toxicities occurred when patients were receiving treatment, and we used this value to determine the rate of toxicities observed during the study. In *Schmoll* et al. the median time duration of exposure to chemotherapy

was 210 days, which was about 70% of the time of median PFS. Since the time of duration was not provided in *Capitain* et al., we estimated that the time of exposure was 11 months (e.g., 70% of the median PFS for that study).

There are multiple limitations of our CUA model. First, CLAUDIA has not been tested in preclinical experiments nor clinical trials to compare its effectiveness to TDM and BSA-based dosing; thus, the estimated RR values that attempt to capture its therapeutic benefit could be incorrect. Second, the lack of a clinical study directly comparing BSA-based treatment and TDM in a FOLFOX regimen and reporting the overall survival and progression free survival curves, required us to select two different studies for both arms of the model. *Capitain* et al. was the best available TDM paper, and thus we chose the BSA-based treatment paper to match this TDM study best. We chose a BSA-based paper that treated patients at similar dates, as that would infer that other elements of the standard of care for metastatic colorectal care would be most comparable.[19] Thus, we choose to use *Schmoll* et al. as the BSA-arm, as the patients were treated within a similar time range (*Schmoll* et al.: 2006–2009, *Capitain* et al.: 2000–2007), patients were selected from 28 different countries, and the clinical trial was a double blind clinical trial.[63] There were other studies that used FOLFOX in the treatment of mCRC that had superior OS of patients than in *Schmoll* et al.,[66,67] but these studies had shortfalls that excluded their use in the CUA; one study required patients to be wild type KRAS,[67] and another study was conducted with an open-label design, was conducted from 2008 to 2012, and was conducted completely in one country.[66] Third, although the cost estimates for CLAUDIA take most aspects of the potential cost of CLAUDIA into account, when the system is implemented clinically this estimate may prove to be incorrect. Fourth, we assume that our system will be used at designated infusion centers and that the patients will require minimal medical attention once the patient is hooked up to the system since everything will be automated. Due to this, we assume the costs associated with being in the infusion center during the infusion is similar to the cost for a hotel room, as we consider the costs of CLAUDIA and healthcare providers separately. Moreover, it is possible that infusion centers specific for CLAUDIA could be built to serve patients being served by this system. Additionally, we assume that the information gained during the first 4 h of cancer treatment is not sufficient to program a wearable pump that the patient could then wear as is used in current clinical practice with a BSA-based dosing schedule. If we were able to program a wearable pump using the information from the first 4 h of the infusion, then we significantly over-estimated the costs for our system in our present model, and therefore underestimated its cost-effectiveness. This is because our system would be able to be used for up to 11-times more patients, as we currently estimate that one CLAUDIA system will be needed for one patient over a 46-h period, and thus if the patients only need our system for 4-h each, then 11-times more patients can use our system, therefore decreasing both the portion of the overhead cost each patient pays and the costs associated with each specific patient (i.e., cost of filters, time spent in the clinic, etc.). Moreover, future work developing miniature HPLC-MS systems may enable CLAUDIA to become wearable, in which case the patient would be able to receive the additional 42-h of chemotherapy at home after going into the clinic for the first 4-h of treatment, as in the BSA and TDM scenarios, thereby also decreasing costs.

We calculated the costs per cycle according to the following equations and the data in Table S4

BSA.

$$cost\ of\ drugs + outpatient\ doctor\ visit + 4\ hours\ infusion\ center\ x\ cost\ per\ hour\ of\ infusion\ center\ chemo + prolonged\ infusion\ at\ home\ with\ pump$$

TDM (PK monitoring). BSA cost + cost of the PK test + nursing cost for 1 h of infusion center work.

A nurse will on average be required to spend an additional 1 h with patients on the TDM (PK monitoring) taking blood and doing other tasks necessary for TDM (PK monitoring).

CLAUDIA group. The costs are the cost of CLAUDIA plus the costs stated in the BSA group, except in the CLAUDIA group the patient does not wear the pump at home.

$$(BSA\ cost - long\ term\ infusion\ at\ home\ with\ pump) + costs\ of\ CLAUDIA$$

Where cost of CLAUDIA (per cycle) equals:

$$\frac{upfront\ system\ cost}{number\ of\ uses\ over\ lifetime} + \frac{annual\ maintence}{number\ of\ annual\ uses} + disposables\ cost + infusion\ center$$

Where the infusion center costs are the costs associated with being a patient in the infusion center.

$$upfront\ system\ cost = cost\ of\left[HPLC + control\ system + infusion\ pump + \frac{sample\ preparation\ device}{4\ patients/device} + \frac{MS}{10\ patients/MS}\right]$$

The cost of the MS and sample preparation device is divided by 10 and 4 patients/device, respectively, because the devices can be used for 10 and 4 patients simultaneously, respectively. Ten patients can be monitored by one MS simultaneously because the 5-FU and 5-BU peaks elute in <0.3 min time frame (see Data S1 Figure 1) and each patient will only have blood sampled every 4 min. Thus, the MS could monitor up to 13 patients simultaneously if the injections are properly staggered, and Agilent sells equipment that can take the samples from multiple different HPLCs simultaneously and place it onto the MS. We conservatively said that each MS could serve 10 patients at a given time. Similarly, the sample preparation method we developed takes ~2 min and has two 30 s centrifuge steps. Thus, if the steps are properly staggered, the same sample preparation device can be used for 4 patients simultaneously.

$$number\ of\ annual\ uses = \frac{365\ days}{2\ days\ per\ chemo\ cycle} x\ percent\ of\ year\ running$$

It was assumed that the machine would run for 75% of the year, giving necessary time for maintenance. I assumed additionally that the device could be used over 15 years, given the regular maintenance that would be performed on the system.

$$number\ of\ uses\ over\ lifetime = number\ of\ annual\ uses\ x\ number\ of\ years\ of\ device\ lifetime$$

$$disposables\ cost = cost\ filters + cost\ solvent$$

$$cost\ filters = cost\ per\ filter\ x\ number\ of\ samples\ per\ chemo\ cycle$$

$$number\ of\ samples\ per\ chemo\ cycle\ =\ 46\ hours\ x\ 15\frac{samples}{hour} = 690\ samples$$

QUANTIFICATION AND STATISTICAL ANALYSIS

We computed metrics quantifying the performance of CLAUDIA in a step response compared to BSA-based dosing to reach the target concentration range of 2.5–3 mg/L. While extracting the time the concentration was below, in, or above the target concentration, only timepoints from time 24-min after the infusion started to the end of the CRI or the end of the step for the CLAUDIA groups was used for the calculation. The 24 min timepoint was chosen because it takes a CRI approximately 4–5 half-lives of the drug to reach steady state, and since we were interested in extracting the metrics evaluating how CLAUDIA performed once the system reached steady state (i.e., and not including when it was increasing toward this point). The area under the curve (AUC) was calculated using data from 24 min to 200 min after the start of the 5-FU infusion by multiplying the measured concentrations by the time spent at each concentration. We summed all these values together for the total AUC. To determine the percent of timepoints that were below, in or above the target range, we counted the number of datapoints that were either below, in or above the target range over this time range and reported the amount of time in each range as the percent of timepoints in that range. We calculated the root mean squared error between the actual and target concentration of 2.75 mg/L. For this metric, we used data from 24-min after the start of the infusion to the end of the step for the CLAUDIA experiments or the end of the CRI for the BSA-groups. For the line plots of deviation from the target concentration versus time, we took the difference between the actual concentration and the target concentration of 2.75 mg/L. We used Python v. 3.10.5 with NumPy v. 1.23.3, Pandas v. 1.4.3, Matplotlib v. 3.5.2, Seaborn v. 0.11.2, and SciPy v. 1.9.0 for analysis and plotting. The statistical test used for each set of data was an independent Student's t test, and is included in the figure caption, including any corrections for multiple tests, as well as the values used for determining significance cutoff values.

Med, Volume *5*

Supplemental information

Closed-loop automated drug infusion regulator:

A clinically translatable, closed-loop

drug delivery system for personalized drug dosing

Louis B. DeRidder, Kyle A. Hare, Aaron Lopes, Josh Jenkins, Nina Fitzgerald, Emmeline MacPherson, Niora Fabian, Josh Morimoto, Jacqueline N. Chu, Ameya R. Kirtane, Wiam Madani, Keiko Ishida, Johannes L.P. Kuosmanen, Naomi Zecharias, Christopher M. Colangelo, Hen-Wei Huang, Makaya Chilekwa, Nikhil B. Lal, Shriya S. Srinivasan, Alison M. Hayward, Brian M. Wolpin, David Trumper, Troy Quast, Douglas A. Rubinson, Robert Langer, and Giovanni Traverso

Supporting Information:

This PDF file includes:

Tables S1 to S4
Figures S1 to S5

Table S1. Method validation results for sample preparation methods. Related to Figure 1. Summary results of the method validation for: (A) the optimal sample preparation method, and (B) the alternative, more rapid sample preparation method. Precision is given as % CV. The recovery is given as the mean ± standard deviation.

A

Lower Limit of Quantification (mg/L)	0.5	
Limit of Detection (LOD) (mg/L)	0.21162	
Linearity Range (mg/L)	0.5 - 40	
Regression Analysis	$y = 0.21005x + 0.0103$ ($r^2 = 0.9967$, $n = 6$)	
Intra-day Accuracy ($n = 6$)	0.5 mg/L	+1.5%
	2 mg/L	−11.6%
	10 mg/L	−11.3%
	40 mg/L	+5.7%
Intra-day Precision ($n = 6$)	0.5 mg/L	13.9%
	2 mg/L	12.6%
	10 mg/L	7.2%
	40 mg/L	11.8%
Inter-day Accuracy (5 days, $n = 30$)	0.5 mg/L	−11.6%
	2 mg/L	−8.0%
	10 mg/L	−3.0%
	40 mg/L	−4.8%
Inter-day Precision (5 days, $n = 30$)	0.5 mg/L	22.5%
	2 mg/L	11.9%
	10 mg/L	12.3%
	40 mg/L	13.7%
Recovery ($n = 6$)	2 mg/L	11.7 ± 2.45%
	10 mg/L	16.3 ± 0.63%
	40 mg/L	20.6 ± 2.75%

B

Lower Limit of Quantification (mg/L)	0.5	
Limit of Detection (LOD) (mg/L)	0.23857	
Linearity Range (mg/L)	0.5 - 40	
Regression Analysis	$y = 0.37810x + 0.017132$ ($r^2 = 0.99771$, $n = 3$)	
Intra-day Accuracy ($n = 6$)	0.5 mg/L	+2.1%
	2 mg/L	+18.7%
	10 mg/L	−5.9%
	40 mg/L	+13.7%
Intra-day Precision ($n = 6$)	0.5 mg/L	15.6%
	2 mg/L	3.8%
	10 mg/L	5.6%
	40 mg/L	7.0%
Calibration Curve Accuracy ($n = 3$)	0.5 mg/L	+16.0%
	2 mg/L	−5.7%
	10 mg/L	−3.4%
	40 mg/L	+2.0%
Calibration Curve Precision ($n = 3$)	0.5 mg/L	9.3%
	2 mg/L	9.5%
	10 mg/L	1.3%
	40 mg/L	2.0%
Recovery ($n = 6$)	2 mg/L	27.5 ± 1.38%
	10 mg/L	26.0 ± 1.53%
	40 mg/L	28.5 ± 2.72%

Table S2. Method validation results over five days for the optimal sample preparation method and for multiple chemotherapies. Related to Figure 1. Results from each of the 5 days for the (A) QCs and (B) calibration curve. (C) Method validation for multiple chemotherapies extracted and analyzed simultaneously in a single method. Precision is given as % CV. The recovery is given as the mean ± standard deviation.

A)

	Day 0		Day 1		Day 2		Day 3		Day 6	
Lower Limit of Quantification (mg/L)	0.5		0.5		0.5		0.5		0.5	
Limit of Detection (LOD) (mg/L)	0.21162		0.27370		0.10126		0.20249		0.24739	
Linearity Range (mg/L)	0.5 - 40		0.5 - 40		0.5 - 40		0.5 - 40		0.5 - 40	
Regression Analysis	$y = 0.21005x + 0.0103$		$y = 0.23231x - 2.004e{-005}$		$y = 0.24640x + 0.0030$		$y = 0.20054x + 6.158e{-004}$		$y = 0.22782x - 0.00407$	
	($r^2 = 0.9967$, $n = 3$)		($r^2 = 0.9924$, $n = 3$)		($r^2 = 0.9954$, $n = 3$)		($r^2 = 0.9925$, $n = 3$)		($r^2 = 0.9841$, $n = 3$)	
	0.5 mg/L	+1.5%	0.5 mg/L	−31.1%	0.5 mg/L	−17.0%	0.5 mg/L	−18.9%	0.5 mg/L	+7.6%
Intra-day Accuracy ($n = 6$)	2 mg/L	−11.6%	2 mg/L	−10.4%	2 mg/L	−21.2%	2 mg/L	+0.9%	2 mg/L	+2.4%
	10 mg/L	−11.3%	10 mg/L	−3.3%	10 mg/L	−17.3%	10 mg/L	+10.2%	10 mg/L	+6.4%
	40 mg/L	+5.7%	40 mg/L	−7.3%	40 mg/L	−17.7%	40 mg/L	+8.7%	40 mg/L	−1.9%
	0.5 mg/L	13.9%	0.5 mg/L	26.4%	0.5 mg/L	8.1%	0.5 mg/L	16.6%	0.5 mg/L	16.8%
Intra-day Precision ($n = 6$)	2 mg/L	12.6%	2 mg/L	5.8%	2 mg/L	2.6%	2 mg/L	3.1%	2 mg/L	8.4%
	10 mg/L	7.2%	10 mg/L	7.7%	10 mg/L	4.4%	10 mg/L	5.9%	10 mg/L	5.1%
	40 mg/L	11.8%	40 mg/L	9.5%	40 mg/L	5.2%	40 mg/L	16.6%	40 mg/L	5.3%

B)

	Day 0		Day 1		Day 2		Day 3		Day 6	
Lower Limit of Quantification (mg/L)	0.5		0.5		0.5		0.5		0.5	
Limit of Detection (LOD) (mg/L)	0.21162		0.27370		0.10126		0.20249		0.24739	
Linearity Range (mg/L)	0.5 - 40		0.5 - 40		0.5 - 40		0.5 - 40		0.5 - 40	
Regression Analysis	$y = 0.21005x + 0.0103$		$y = 0.23231x - 2.004e{-005}$		$y = 0.24640x + 0.0030$		$y = 0.20054x + 6.158e{-004}$		$y = 0.22782x - 0.00407$	
	($r^2 = 0.9967$, $n = 3$)		($r^2 = 0.9924$, $n = 3$)		($r^2 = 0.9954$, $n = 3$)		($r^2 = 0.9925$, $n = 3$)		($r^2 = 0.9841$, $n = 3$)	
	0.5 mg/L	+7.0%	0.5 mg/L	−11.1%	0.5 mg/L	+3.9%	0.5 mg/L	−15.3%	0.5 mg/L	−10.2%
Calibration Curve Accuracy ($n = 3$)	2 mg/L	−5.9%	2 mg/L	+4.6%	2 mg/L	−1.5%	2 mg/L	−1.5%	2 mg/L	+6.8%
	10 mg/L	−0.1%	10 mg/L	+8.3%	10 mg/L	−3.4%	10 mg/L	+2.6%	10 mg/L	−15.3%
	40 mg/L	−1.0%	40 mg/L	−5.4%	40 mg/L	−1.2%	40 mg/L	−5.6%	40 mg/L	−6.1%
	0.5 mg/L	11.8%	0.5 mg/L	12.3%	0.5 mg/L	18.3%	0.5 mg/L	15.6%	0.5 mg/L	30.5%
Calibration Curve Precision ($n = 3$)	2 mg/L	13.2%	2 mg/L	4.8%	2 mg/L	6.9%	2 mg/L	10.4%	2 mg/L	8.4%
	10 mg/L	6.3%	10 mg/L	5.1%	10 mg/L	4.7%	10 mg/L	7.5%	10 mg/L	2.5%
	40 mg/L	3.8%	40 mg/L	3.3%	40 mg/L	3.5%	40 mg/L	6.3%	40 mg/L	6.6%

C)

	Irinotecan Hydrochloride		Theophylline		Thiotepa		Cyclophosphamide		Doxorubicin Hydrochloride	
Limit of Quantification (mg/L)	0.5		0.5		0.5		0.8		0.8	
Linearity Range (mg/L)	0.5 - 60		0.5 - 60		0.5 - 60		0.8 - 60		0.8 - 60	
Regression Analysis	$y = 0.6805x - 0.0451$		$y = 0.07496x + 0.0168$		$y = 0.1379x - 2.129e{-003}$		$y = 0.1857x + 0.0211$		$y = 0.08379x - 0.0091$	
	($r^2 = 0.9965$, $n = 3$)		($r^2 = 0.9961$, $n = 3$)		($r^2 = 0.9664$, $n = 3$)		($r^2 = 0.9860$, $n = 3$)		($r^2 = 0.9931$, $n = 3$)	
Calibration Curve Accuracy ($n = 3$)	0.5 mg/L	+14.9%	0.5 mg/L	+17.2%	0.5 mg/L	+29.1%	0.5 mg/L	N/A	0.5 mg/L	N/A
	10 mg/L	−3.2%	10 mg/L	+10.5%	10 mg/L	+4.0%	10 mg/L	+16.1%	10 mg/L	−20.4%
	40 mg/L	−2.3%	40 mg/L	−0.8%	40 mg/L	−1.0%	40 mg/L	−8.7%	40 mg/L	−0.2%
Calibration Curve Precision ($n = 3$)	0.5 mg/L	10.7%	0.5 mg/L	37.4%	0.5 mg/L	6.9%	0.5 mg/L	N/A	0.5 mg/L	N/A
	10 mg/L	4.2%	10 mg/L	9.5%	10 mg/L	20.5%	10 mg/L	5.4%	10 mg/L	13.7%
	40 mg/L	1.7%	40 mg/L	2.6%	40 mg/L	21.7%	40 mg/L	8.3%	40 mg/L	21.8%
Intra-Day Accuracy ($n = 6$)	50 mg/L	−6.3%	50 mg/L	+15.1%	50 mg/L	+45.4%	50 mg/L	+17.6%	50 mg/L	−11.2%
Intra-Day Precision ($n = 6$)	50 mg/L	3.1%	50 mg/L	2.5%	50 mg/L	0.8%	50 mg/L	2.6%	50 mg/L	33.6%
All Chemos Mixed Accuracy (n = 6)	10 mg/L	−22.3%	10 mg/L	−0.2%	10 mg/L	+28.0%	10 mg/L	+21.6%	10 mg/L	−38.8%
	30 mg/L	−18.6%	30 mg/L	−2.1%	30 mg/L	+21.2%	30 mg/L	+9.0%	30 mg/L	−9.2%
All Chemos Mixed Precision ($n = 6$)	10 mg/L	6.6%	10 mg/L	3.8%	10 mg/L	3.1%	10 mg/L	2.9%	10 mg/L	38.0%
	30 mg/L	5.6%	30 mg/L	3.0%	30 mg/L	6.8%	30 mg/L	3.1%	30 mg/L	4.9%

Table S3. Model parameters for the cost-effectiveness model. Related to Figure 4.

Parameter	Base Case Value	Range used for sensitivity analysis	Reference(s)
Overall parameters			
Starting age (years)	62		[S1,S2]
Sex	Male and Female		[S1,S2]
Discount rate	0.03	0-0.05	Both costs and effectiveness [S3]
Utilities			
FOLFOX	0.85	0.68-1	[S4]
Progressed	0.65	0.52-0.78	[S4]
Dead	0		
Disutilities			
Diarrhea	-0.36	-0.43 to -0.29	[S4]
Fibromyalgia	-0.45	-0.54 to -0.36	[S4]
Mucositis	-0.087	-0.182 to 0	[S5]
Neutropenia	-0.090	-0.119 to -0.060	[S6]
Overall costs per cycle†			
On FOLFOX			
BSA	957.95	731.03-1170.71	
TDM	1465.19	1110.03-1813.71	
CLAUDIA	1774	1226-2469	
Progressed from FOLFOX to FOLFIRI			
BSA	906.64	689.98-1109.14	
TDM	1413.88	1068.98-1752.14	
CLAUDIA	1723	1185-2407	
Costs for Grade 3/4 Toxicities			
Fibromyalgia	13,647	8,368-32,632	[S4, S7]
Diarrhea	84	67-101	[S4]

Mucositis	5,976	2,822-9,960	S8
Neutropenia	24,518.04	14,973-29,228	S9
Probability of grade 3/4 toxicities			
BSA Arm (over 210 days)			
Diarrhea	0.12	0.003-0.15	S1, S4
Fibromyalgia	0.04	0.011-0.0136	S4
Mucositis	0.15	0.03-0.15	S1, S10
Neutropenia	0.25	0.24-0.29	S1, S2, S11
TDM Arm (over 11 months)			
Diarrhea	0.017	0.003-0.102	S1, S4
Fibromyalgia	0.013	0.002-0.051	S4
Mucositis	0.008	0 – 0.15	S1
Neutropenia	0.18	0.17 – 0.29	S1
Rate of death per year			
BSA			
Months 0-9	0.125748		
9+	0.533161		
TDM			
Months 0-11	0.133274		
11+	0.375066		
Rate of progression per year			
BSA			
Months 0-6.9	0.747251583		
6.9-15.7	1.207248863		
15.7+	1.758805844		
TDM			
Months 0-7.5	0.260030287		
7.5-20	0.627769409		
20+	0.07073301		
Relative Risk (RR) for Closed-loop Arm (compared to the TDM arm) for:			
Toxicities	0.75	0.25-1	
PFS	0.75	0.25-1	
OS	0.85	0.25-1	

†: all values were adjusted from their reported USD to 2019 USD

[a]: Quote from supplier

Table S4. Costs of multiple items used to estimate costs of BSA, TDM, and CLAUDIA groups. Related to Figure 4. The supplementary methods described how these values were combined to estimate the overall cost per cycle of the different treatment groups.

Costs per cycle of chemotherapy†			
FOLFOX drugs	443.91	355.13-532.69	[S4,S12]
FOLFIRI drugs	392.60	314.08-471.12	[S4,S12]
First hour of chemo	169.04	117.35-224.93	[S4]
Additional hour of chemo	36.13	26.79-46.61	[S4]
Long term infusion with pump at home	178	127.11-195	[S13]
Nurse salary per hour	35.24	25-53	[S14]
PK Test	400	300-500	[S4]
Costs for CLAUDIA			
Cost of CLAUDIA per use	994	622-1493	Estimated described in detail in the Supplemental Methods
Costs used to estimate the cost of CLAUDIA			
HPLC with autosampler	150,000	75,000-200,000	
Mass spec with ESI	500,000	350,000-700,000	
Automated sample preparation device	150,000	25,000-250,000	
Cost of controller and infusion pump	1,000	750-3,000	
Annual maintenance cost	50,000	30,000-70,000	
Cost per patient			
Cost of each filter	0.19	0.10-0.24	Applied 60% discount to research grade price for 100 filters to get to an estimated bulk price
Solvent cost per cycle	31.70	26.42-52.84	Estimated based on the flow rate of the HPLC system over 46 hours
Cost of staying at infusion center for the infusion	350	250-600	

†: all values were adjusted from their reported USD to 2019 USD

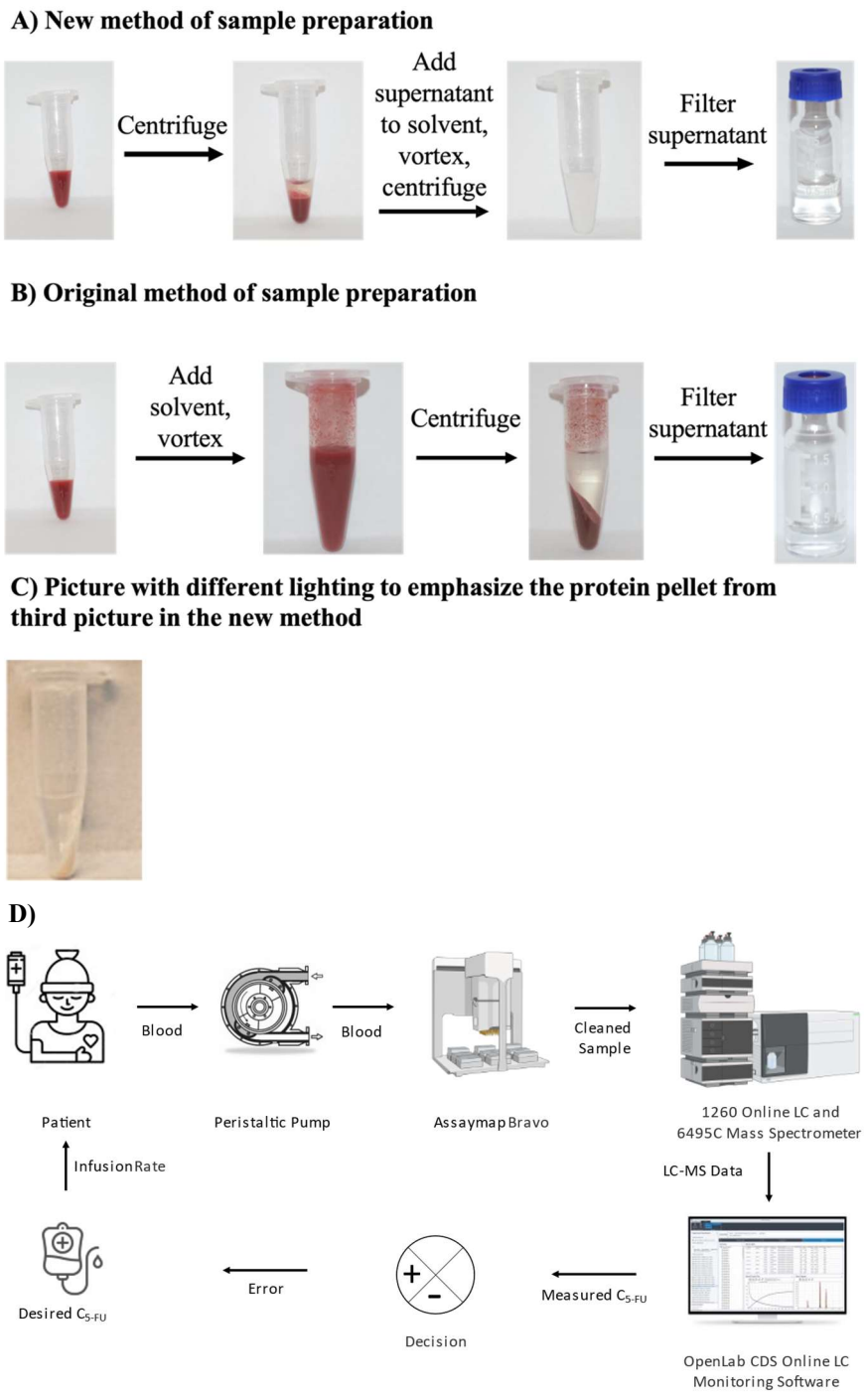

Figure S1. Rapid sample preparation methods in CLAUDIA, and proposed version of an automated CLAUDIA. Related to Figure 1. (A) The optimized procedure for sample preparation. (B) An alternative method for sample preparation, which takes slightly less time than the optimized procedure. (C) Same picture as the third from the left that is shown in A with different lighting to demonstrate that there is a protein pellet that formed during this step. (D) Potential version of a fully automated CLAUDIA system.

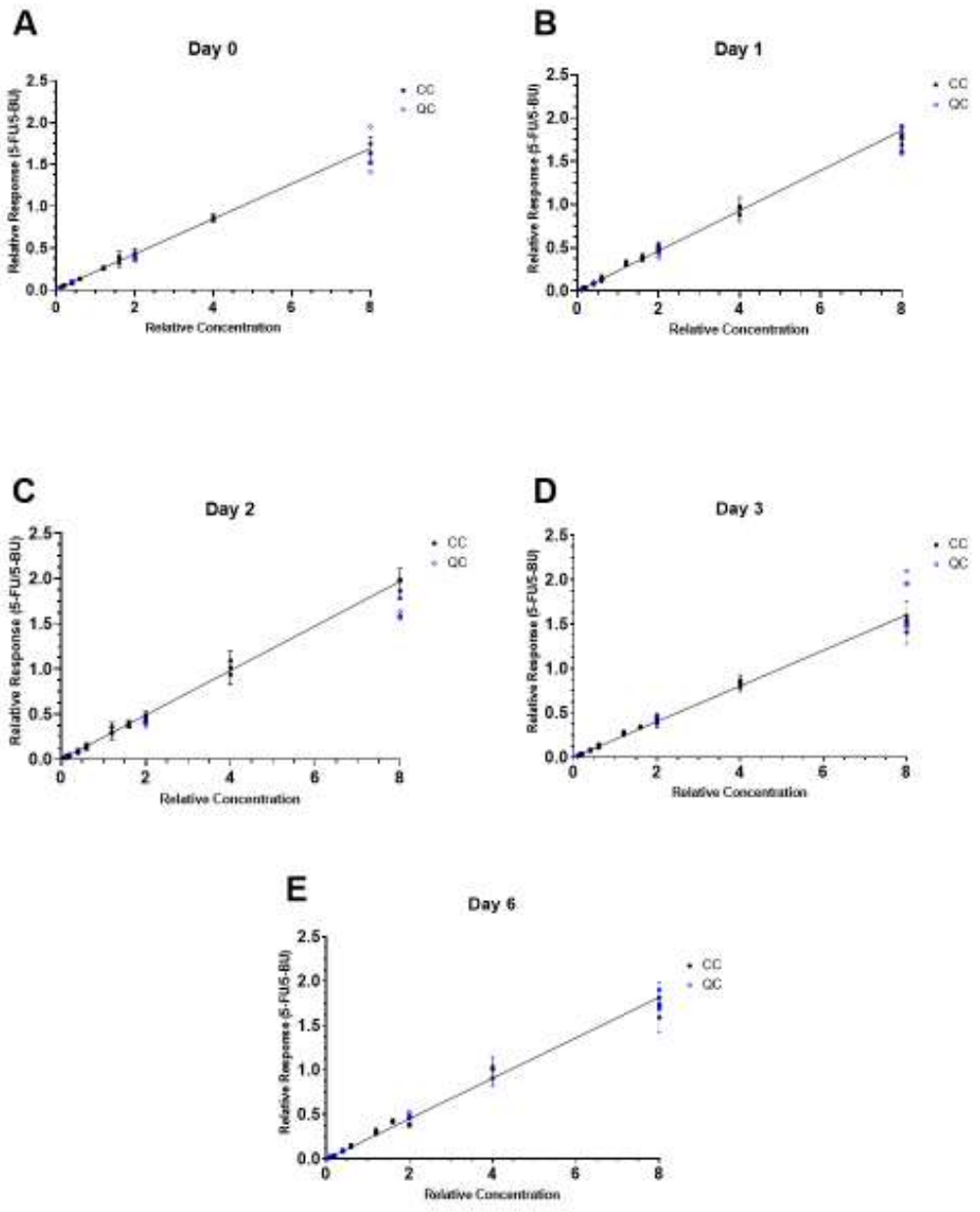

Figure S2. Calibration curves from the 5 days of the method validation of the optimal method (from Figure S1A). Related to Figure 1. Calibration curve datapoints (black, N=3) and QC datapoints (blue, N=6) are shown. 95% confidence interval of the CC points is shown, as well as the linear line of best fit. Graphs were created with GraphPad PRISM v9.5.0.

A

$$c = \frac{g_o}{\tau s + 1} \xrightarrow{\text{Infusion rate (µl/sec)}} c = u * g_o(1 - e^{-\frac{t}{\tau}})$$

Continuous rate infusion experiment number	g_0 (SS gain) $(\frac{s*mg}{L*\mu L})$	τ (min)	τ (sec)
1	1.68	14.06	843.6
2	2.51	1.54	92.4
3	3.26	5.11	306.6

B

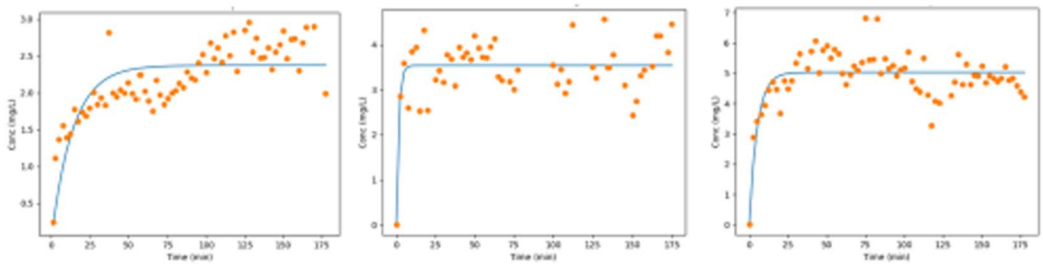

C

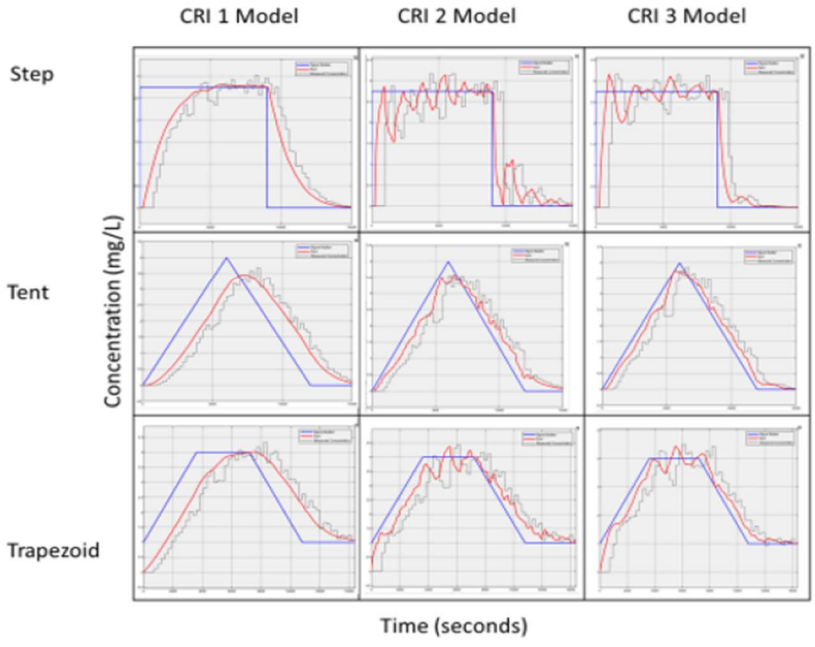

Figure S3. Fitting a PK model to the rabbits and simulations of CLAUDIA. Related to Figures 2 and 3. (A) Model and model parameters for the rabbit PK extracted from the continuous rate infusions used to tune the controller. (B) Overlay of the data from the CRIs and the model fits. (C) Results from SIMULINK simulations. The blue line is the desired setpoint. The red line is the simulated output concentration. The dashed line is the measured concentration, which is the actual concentration with noise and the delay time added.

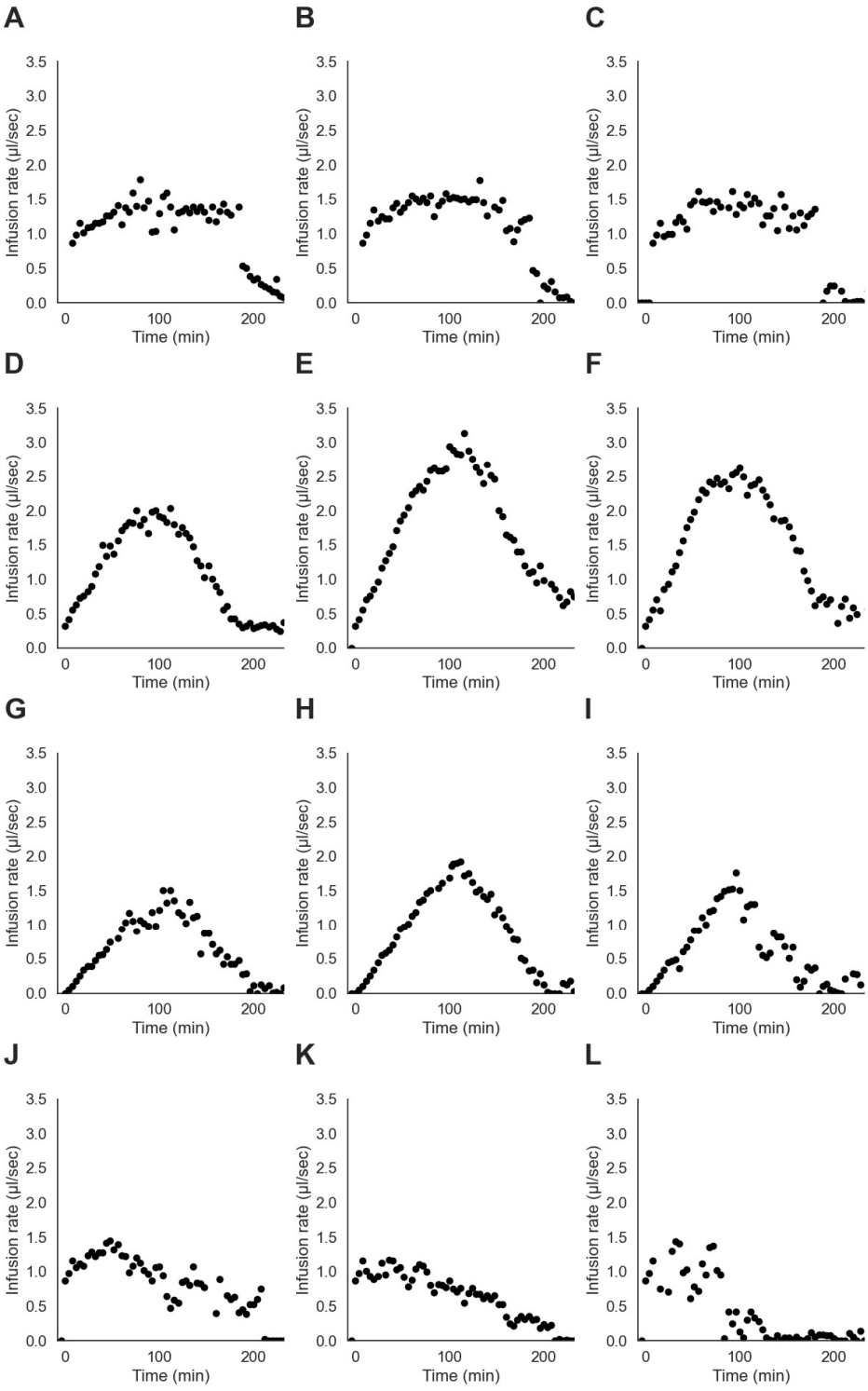

Figure S4. Infusion rates for the CLAUIA experiments. Related to Figures 2 and 3. (A-I) Infusion rates for the (A-C) step. (D-F) tent, and (G-I) trapezoid setpoint experiments with CLAUDIA experiments in Figure 2. (J-L) Infusion rates for the CLAUDIA experiments in Figure 3.

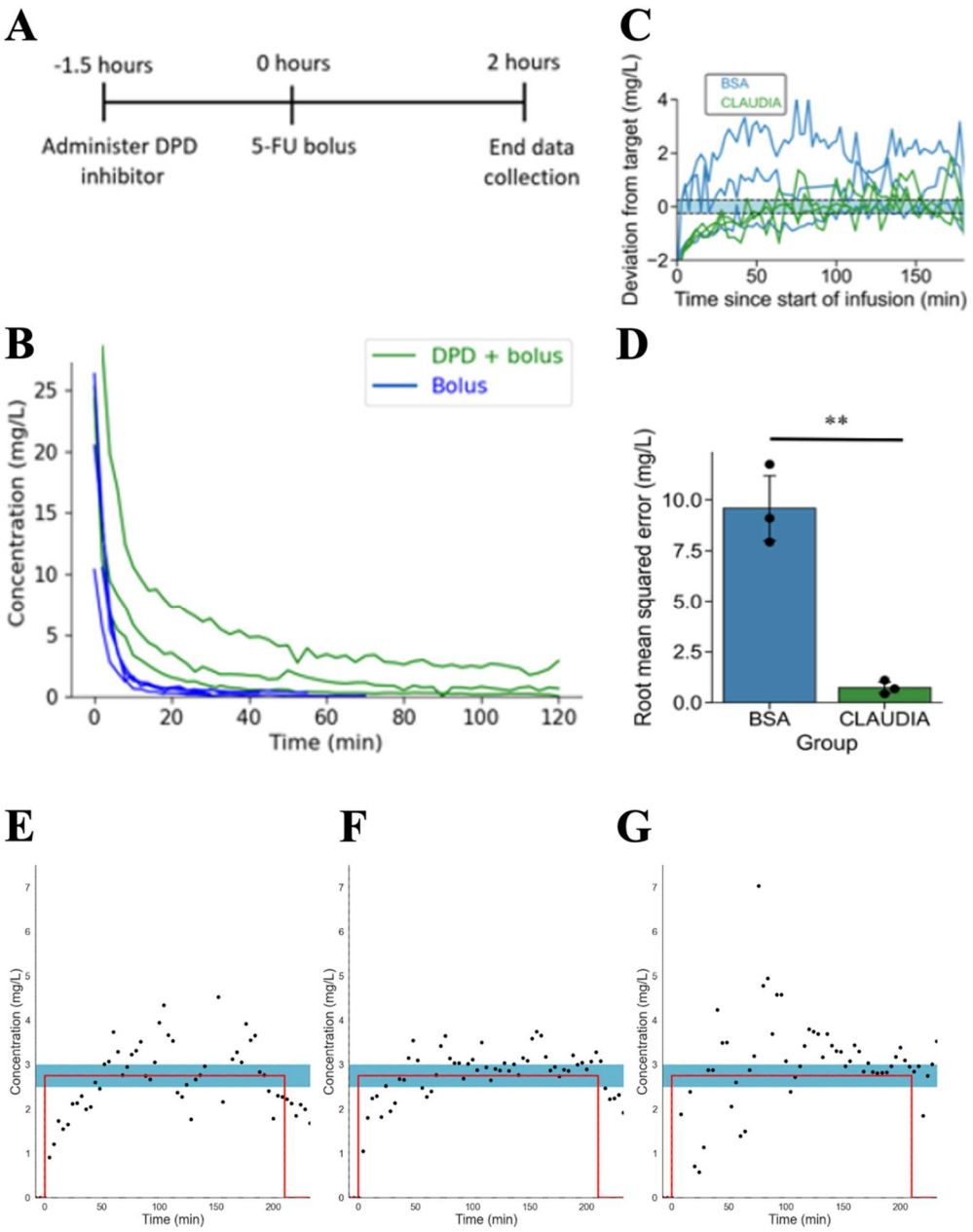

Figure S5. Impact of DPD inhibitor on 5-FU pharmacokinetics given as a bolus and zoomed in view of the results of the CLAUDIA disturbance experiments. Related to Figures 2 and 3. (A) Schematic of rabbit, bolus experiment. (B) Bolus PK data. Data is represented as a line plot, where data points from a single bolus are connected by straight lines. N=3 in the DPD + bolus group. N=4 in the bolus alone group. (C) Deviation from the target concentration of 2.75 mg/L for when the CRI was administered in the BSA group and for the entirety of the step in the CLAUDIA group from Figure 2. The time is the time since the infusion started, as the CLAUDIA group's step function did not increase in concentration until 8 minutes into the experiment. The target range is given by the shaded blue region between –0.25 and 0.25 mg/L. (D) Root mean squared error from the target concentration of 2.75 mg/L for the BSA (N=3) and CLAUDIA groups (N=3) from Figure 3. **: $p<0.01$. Data is mean ± standard deviation. (E-G) Data from CLAUDIA group in Figure 3 represented with a zoom in on the y-axis to allow better visualization of the data.

SI References:

S1. Capitain, O., Asevoaia, A., Boisdron-Celle, M., Poirier, A.-L., Morel, A., and Gamelin, E. (2012). Individual fluorouracil dose adjustment in FOLFOX based on pharmacokinetic follow-up compared with conventional body-area-surface dosing: a phase II, proof-of-concept study. Clin. Colorectal Cancer *11*, 263–267. 10.1016/j.clcc.2012.05.004.

S2. Schmoll, H.-J., Cunningham, D., Sobrero, A., Karapetis, C.S., Rougier, P., Koski, S.L., Kocakova, I., Bondarenko, I., Bodoky, G., Mainwaring, P., et al. (2012). Cediranib with mFOLFOX6 versus bevacizumab with mFOLFOX6 as first-line treatment for patients with advanced colorectal cancer: a double-blind, randomized phase III study (HORIZON III). J. Clin. Oncol. Off. J. Am. Soc. Clin. Oncol. *30*, 3588–3595. 10.1200/JCO.2012.42.5355.

S3. Sanders, G.D., Neumann, P.J., Basu, A., Brock, D.W., Feeny, D., Krahn, M., Kuntz, K.M., Meltzer, D.O., Owens, D.K., Prosser, L.A., et al. (2016). Recommendations for Conduct, Methodological Practices, and Reporting of Cost-effectiveness Analyses: Second Panel on Cost-Effectiveness in Health and Medicine. JAMA *316*, 1093–1103. 10.1001/jama.2016.12195.

S4. Goldstein, D.A., Chen, Q., Ayer, T., Howard, D.H., Lipscomb, J., Harvey, R.D., El-Rayes, B.F., and Flowers, C.R. (2014). Cost Effectiveness Analysis of Pharmacokinetically-Guided 5-Fluorouracil in FOLFOX Chemotherapy for Metastatic Colorectal Cancer. Clin. Colorectal Cancer *13*, 219–225. 10.1016/j.clcc.2014.09.007.

S5. Hagiwara, Y., Shiroiwa, T., Shimozuma, K., Kawahara, T., Uemura, Y., Watanabe, T., Taira, N., Fukuda, T., Ohashi, Y., and Mukai, H. (2018). Impact of Adverse Events on Health Utility and Health-Related Quality of Life in Patients Receiving First-Line Chemotherapy for Metastatic Breast Cancer: Results from the SELECT BC Study. Pharmacoeconomics *36*, 215–223. 10.1007/s40273-017-0580-7.

S6. Zeng, X., Wan, X., Peng, L., Peng, Y., Ma, F., Liu, Q., and Tan, C. (2019). Cost-effectiveness analysis of pembrolizumab plus chemotherapy for previously untreated metastatic non-small cell lung cancer in the USA. BMJ Open *9*, e031019. 10.1136/bmjopen-2019-031019.

S7. Sicras-Mainar, A., Rejas, J., Navarro, R., Blanca, M., Morcillo, Á., Larios, R., Velasco, S., and Villarroya, C. (2009). Treating patients with fibromyalgia in primary care settings under routine medical practice: a claim database cost and burden of illness study. Arthritis Res. Ther. *11*, R54. 10.1186/ar2673.

S8. Elting, L.S., Cooksley, C.D., Chambers, M.S., and Garden, A.S. (2007). Risk, outcomes, and costs of radiation-induced oral mucositis among patients with head-and-neck malignancies. Int. J. Radiat. Oncol. Biol. Phys. *68*, 1110–1120. 10.1016/j.ijrobp.2007.01.053.

S9. Tai, E., Guy, G.P., Dunbar, A., and Richardson, L.C. (2017). Cost of Cancer-Related Neutropenia or Fever Hospitalizations, United States, 2012. J. Oncol. Pract. *13*, e552–e561. 10.1200/JOP.2016.019588.

S10. Yamazaki, K., Nagase, M., Tamagawa, H., Ueda, S., Tamura, T., Murata, K., Eguchi Nakajima, T., Baba, E., Tsuda, M., Moriwaki, T., et al. (2016). Randomized phase III study of bevacizumab plus FOLFIRI and bevacizumab plus mFOLFOX6 as first-line treatment for patients with metastatic colorectal cancer (WJOG4407G). Ann. Oncol. Off. J. Eur. Soc. Med. Oncol. *27*, 1539–1546. 10.1093/annonc/mdw206.

S11. Venook, A.P., Niedzwiecki, D., Lenz, H.-J., Innocenti, F., Fruth, B., Meyerhardt, J.A., Schrag, D., Greene, C., O'Neil, B.H., Atkins, J.N., et al. (2017). Effect of First-Line Chemotherapy Combined With Cetuximab or Bevacizumab on Overall Survival in Patients With KRAS Wild-Type Advanced or Metastatic Colorectal Cancer: A Randomized Clinical Trial. JAMA *317*, 2392–2401. 10.1001/jama.2017.7105.

S12. 2013 ASP Drug Pricing Files | CMS https://www.cms.gov/Medicare/Medicare-Fee-for-Service-Part-B-Drugs/McrPartBDrugAvgSalesPrice/2013ASPFiles.

S13. Physician Fee Schedule Search Results https://www.cms.gov/apps/physician-fee-schedule/search/search-results.aspx?Y=0&T=0&HT=0&CT=3&H1=96416&M=1.
S14. Registered Nurses : Occupational Outlook Handbook: : U.S. Bureau of Labor Statistics https://www.bls.gov/ooh/healthcare/registered-nurses.htm.

Data S1. CLAUDIA validation, performance, and cost-effectiveness modeling. Related to Figures 1, 3, and 4

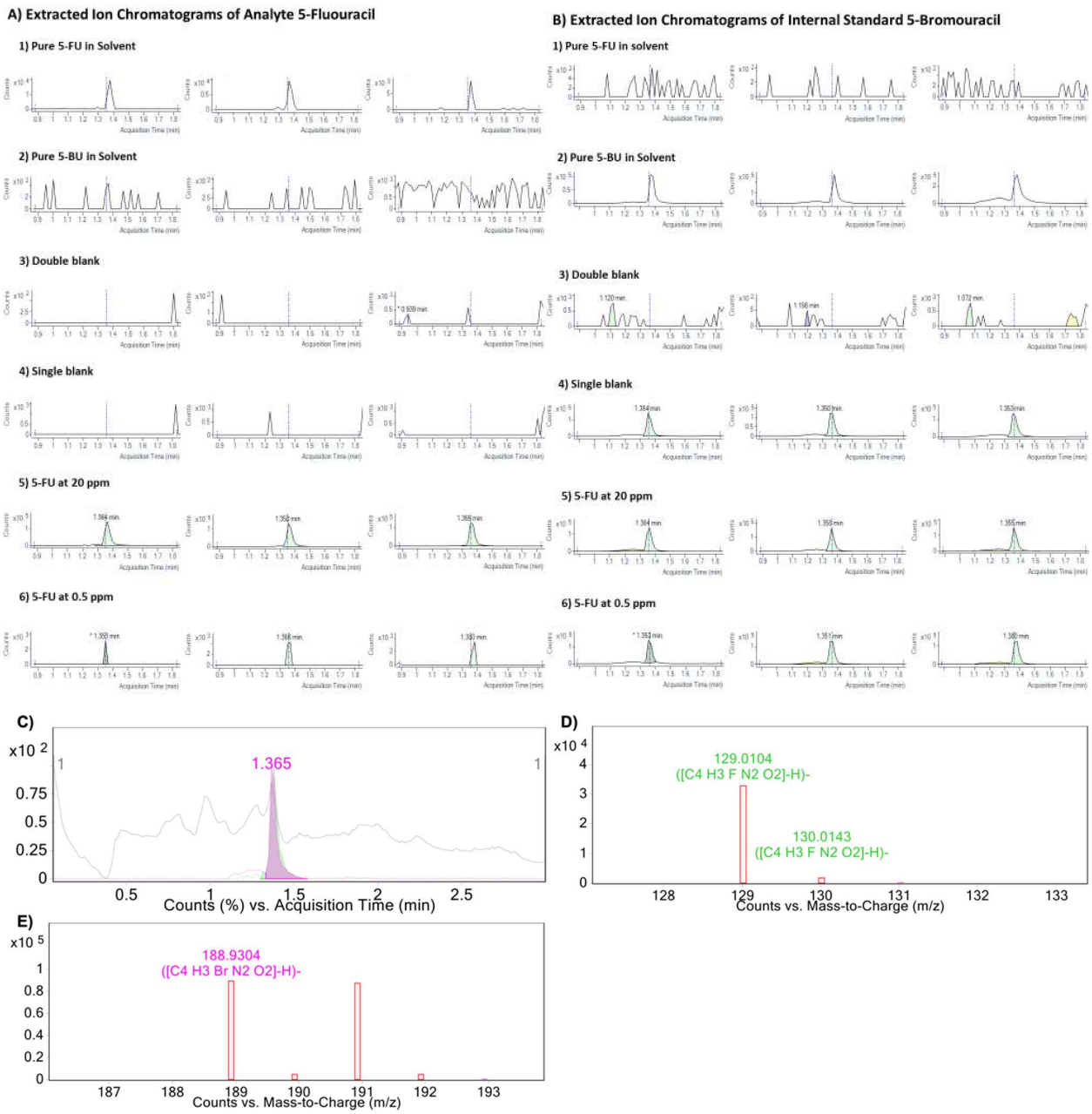

Data S1 Figure 1. Example chromatograms and mass spectra. Related to Figure 1. The extracted ion is (A) 5-FU, and (B) 5-BU. (C-E) Chromatographic separation and TOF detection of 5-FU and 5-BU taken from time point 104 min during one sample rabbit experiment. C) The extracted ion chromatograms (EICs) of 5-FU (green) and 5-BU (magenta) extracted at their theoretical $[M-H]^-$ *m/z* values, with a 50 ppm error tolerance, overlaid on the TIC and normalized to the largest chromatographic peak intensities. D and E) Mass spectra of 5-FU and 5-BU with theoretical *m/z* and isotopic peak intensities overlaid in red boxes. Chromatographic separation and TOF's accurate mass selectivity enable rapid analysis in a complex matrix.

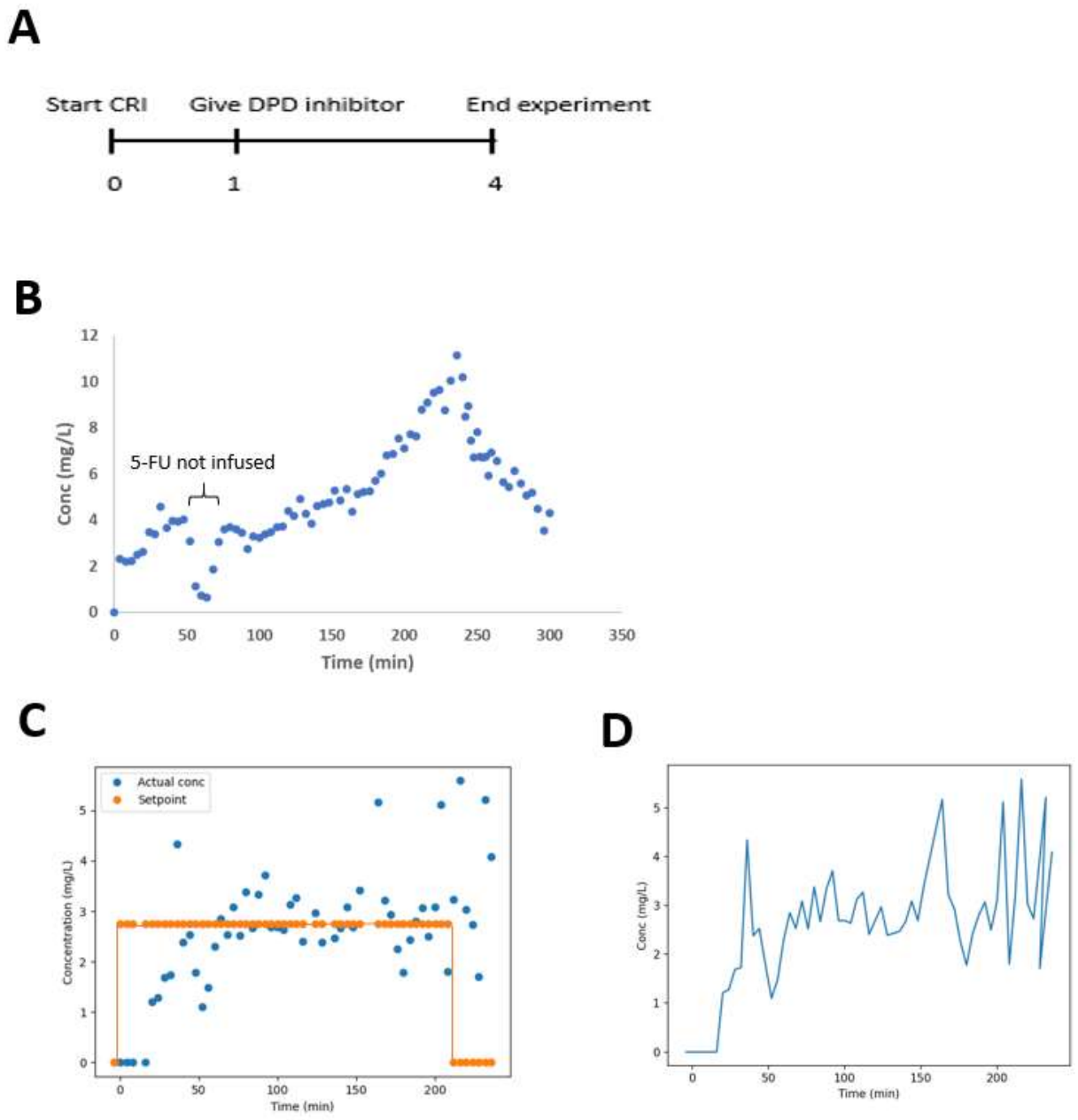

Data S1 Figure 2. Preliminary experiment used to guide design of the controller. Related to Figure 3. (A) Schematic of the experiment. (B) Continuous rate infusion determined by BSA following the scheme in A (N=1). The pump turned off around T50, which resulted in no 5-FU being infused during this interval. Thus, the datapoints from times ~45-75 minutes were artificially low because the pump malfunctioned during that time and did not infuse the drug. (C and D) Preliminary (N=1) CLAUDIA disturbance experiment that informed our design of the controller.

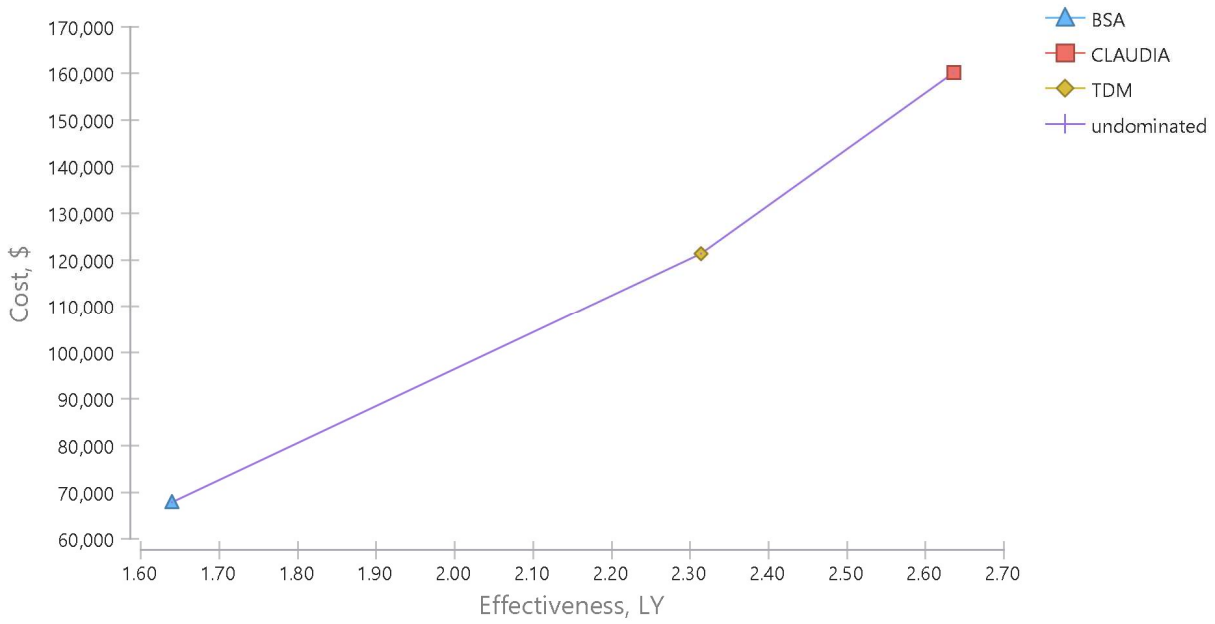

Data S1 Figure 3. Cost-effectiveness plot of the BSA, TDM and CLAUDIA arms. Related to Figure 4. The model was simulated using the base case values for all the parameters given in Table S1, and the overall effectiveness (QALY) and cost (USD) for the BSA, TDM (i.e. PK Monitoring), and the CLAUDIA strategies were calculated and plotted. The slope of the cost-effectiveness plot is the incremental cost-effectiveness ratio (ICER) between the two strategies compared.

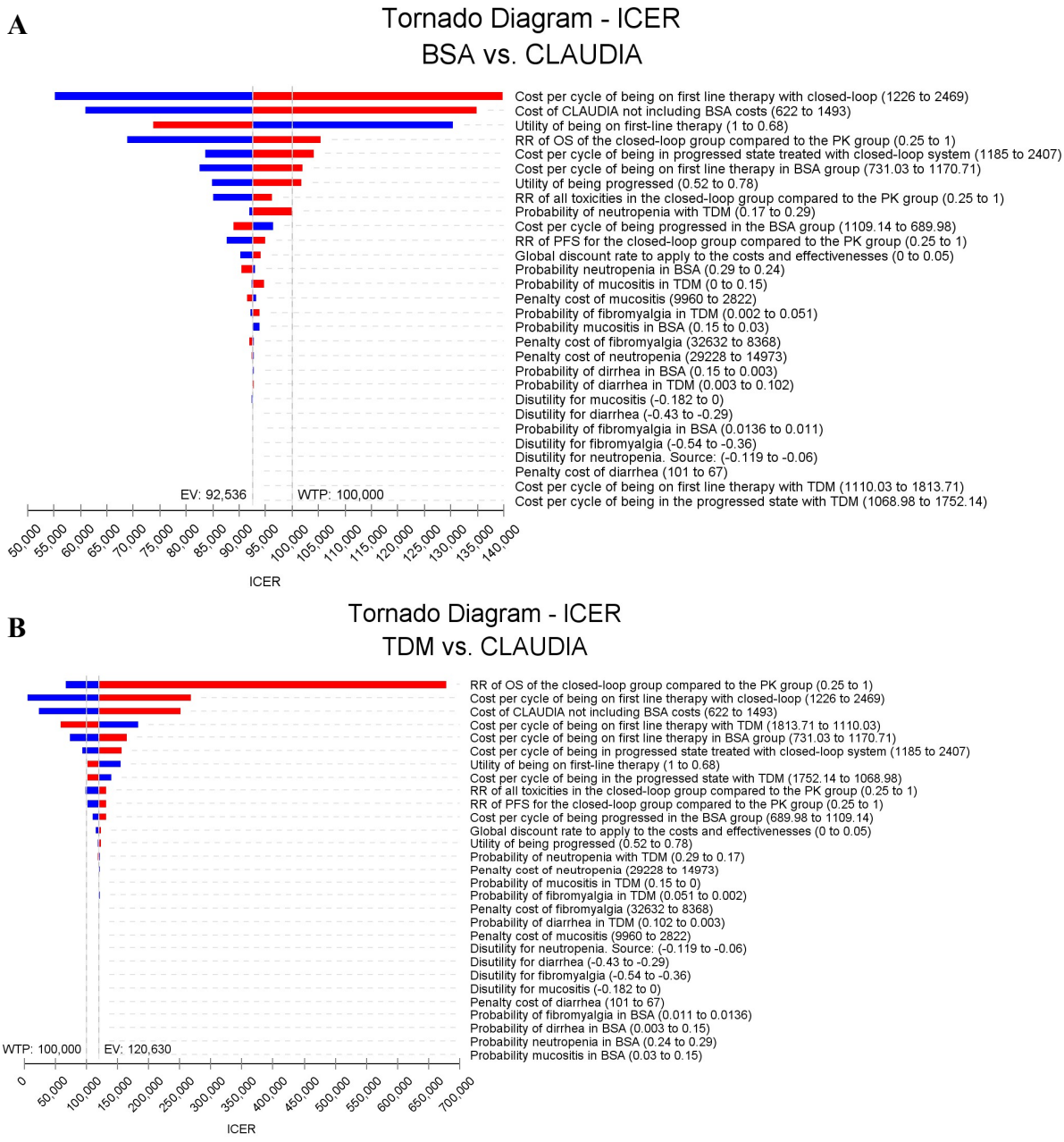

Data S1 Figure 4. Tornado diagram of one-way sensitivity analyses performed on all parameters in our model of (A) CLAUDIA compared to the BSA strategy, and (B) CLAUDIA compared to the TDM strategy. Related to Figure 4. One-way sensitivity analyses were performed for all parameters in the model over the values stated in Table S1, and the impact of changing each of the parameters on the ICER of the CLAUDIA arm compared to (A) the BSA arm and (B) the TDM arm are given in the Tornado plots. (A and B) The cost per cycle of the closed-loop system for a patient on either first-line therapy or in the progressed state includes the costs included in the BSA-based dosing, and the range of parameters included in the sensitivity analysis for these parameters as described in the Supplemental Methods. The "cost of CLAUDIA not using BSA costs" is the cost of using CLAUDIA per cycle (for both patients in state disease and progressed states), without considering the costs associated with the BSA group.

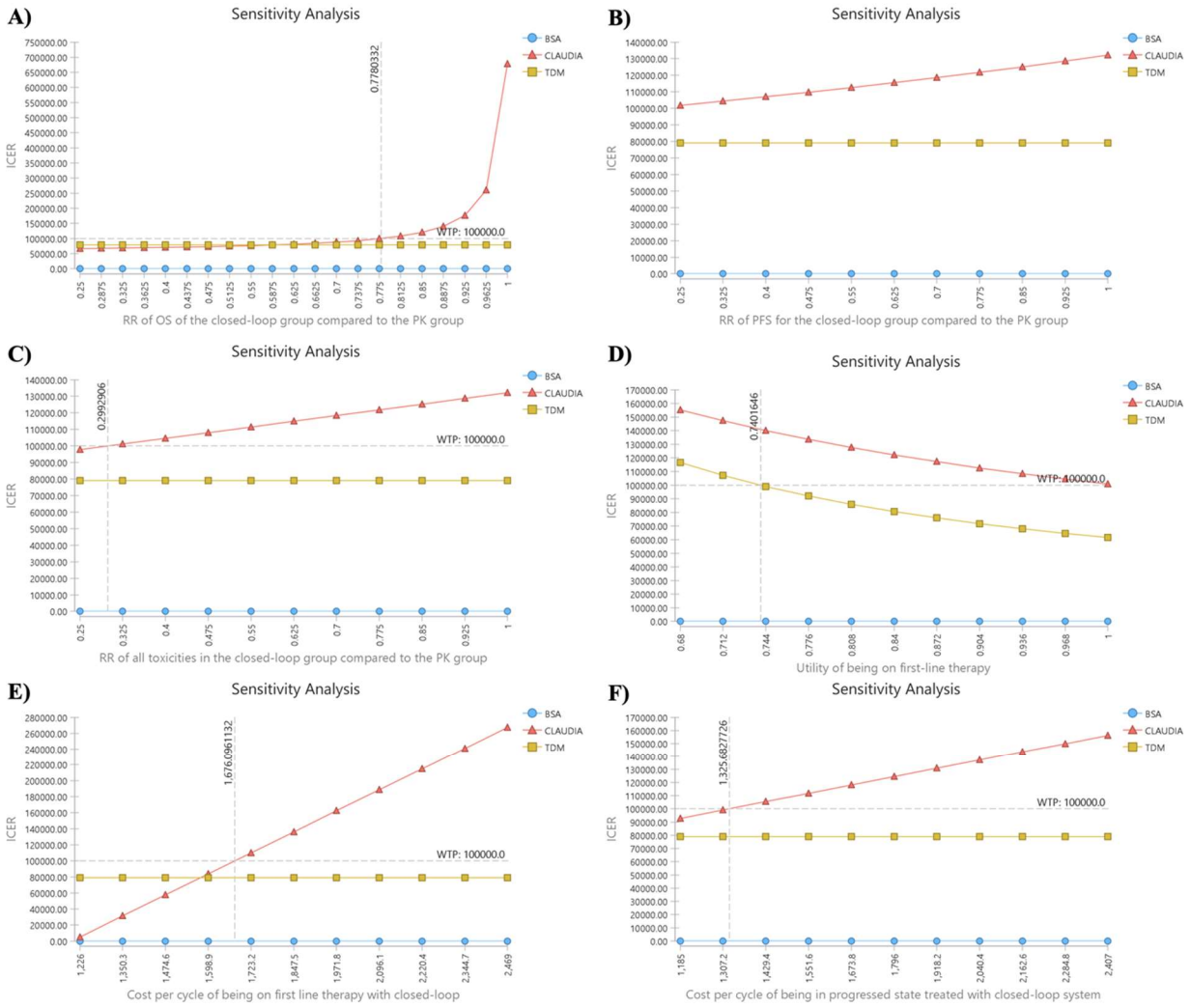

Data S1 Figure 5. One-way sensitivity analyses of the CUA model. Related to Figure 4. Shown for all is the ICER of CLAUDIA vs TDM. (A-C) Sensitivity analysis of relative rates (RR) used between the TDM and CLAUDIA groups with changing the RR for (A) OS, (B) PFS, and (C) Toxicities. Note the TDM and BSA arms did not change as a function of the RR values because the RR values were not included in any of the parameters for those groups. (D) One-way sensitivity analysis on the utility of being on first-line therapy. Sensitivity analysis on the composite costs (e.g., costs of using CLAUDIA per cycle in addition to shared costs with the BSA group) of using CLAUDIA in (E) the stable disease state (i.e., first line therapy) and (F) when in the progressed state. The ICER for CLAUDIA is compared to the TDM group, and not BSA group, in all plots.

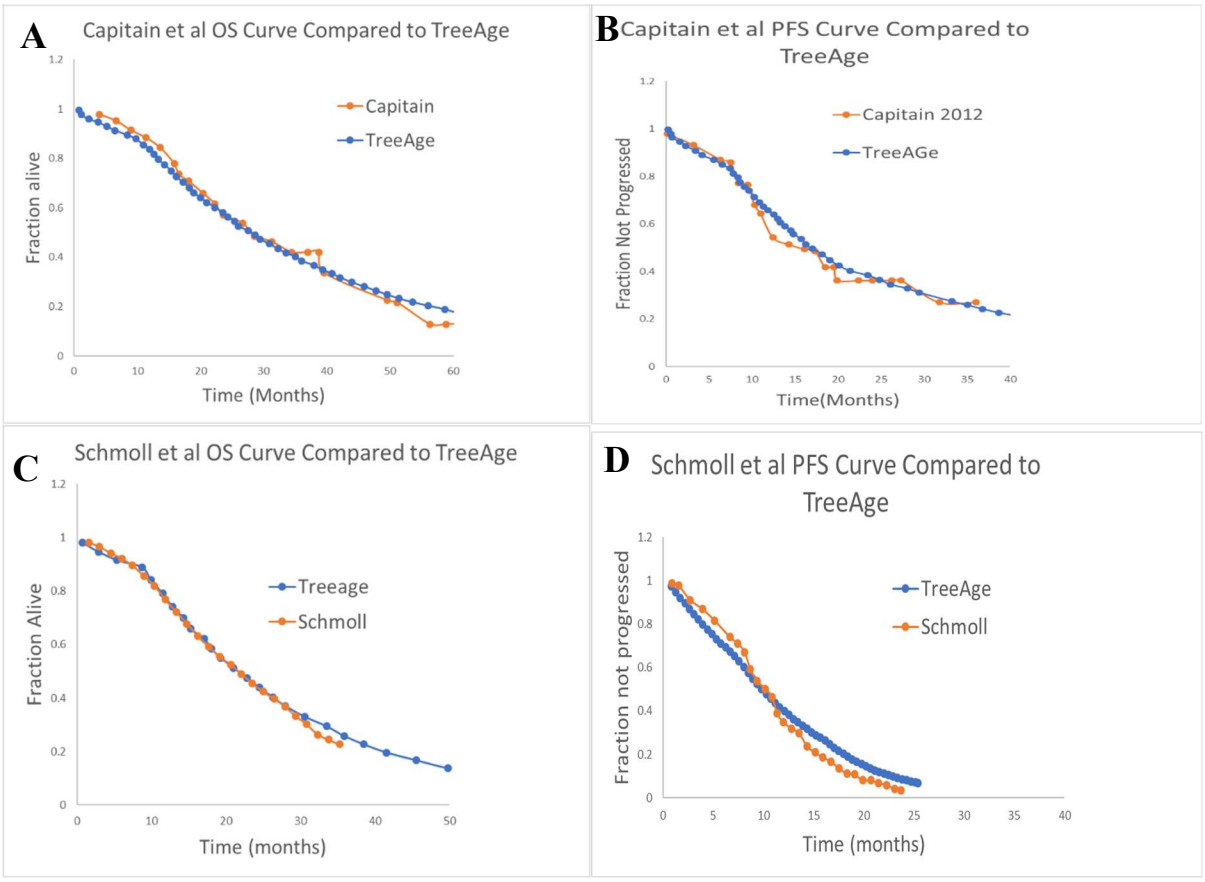

Data S1 Figure 6. Internal validation of PFS and OS curves generated in TreeAge compared to the original paper data. Related to Figure 4. Both overall survival (OS) and progression free survival (PFS) curves were generated in TreeAge using the BSA and TDM arms of the model (blue curves) and were compared to the actual data (orange lines). *Capitain et al*. was the data source for the TDM arm, and *Schmoll et al*. was the data for the BSA arm.

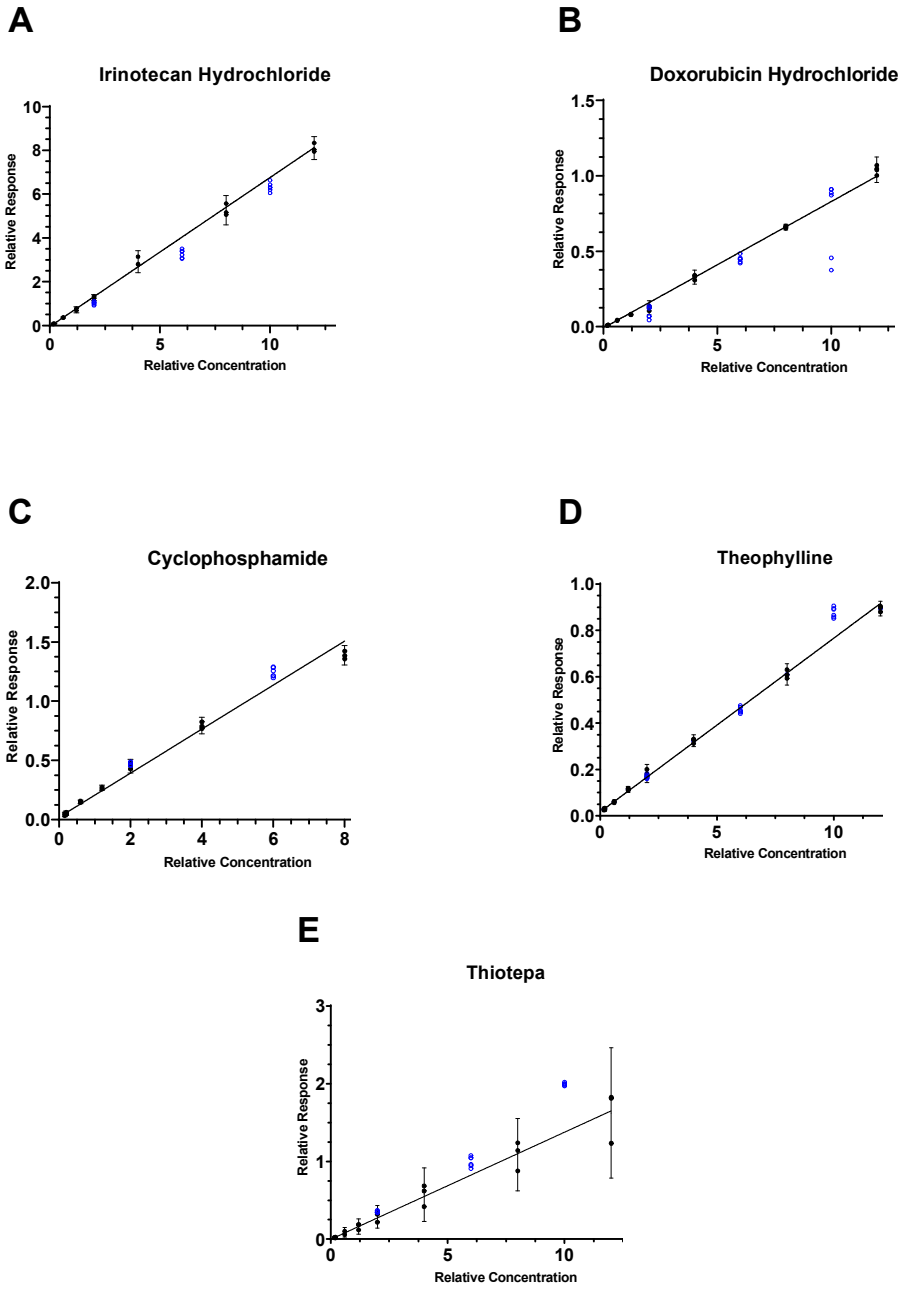

Data S1 Figure 7. Multiple chemotherapies extracted in a single analysis method validation. Related to discussion section and Figure 1. (A) Summary of the results, and (B) the calibration curves and QC values plotted. Graphs were created with GraphPad PRISM v9.5.0.